Journal of Materials Chemistry C

ROYAL SOCIETY OF CHEMISTRY

REVIEW

Cite this: *J. Mater. Chem. C*, 2020, **8**, 12739

Lanthanide-functionalized metal–organic frameworks as ratiometric luminescent sensors

Yifang Zhao and Dan Li *

Received 20th July 2020,
Accepted 12th August 2020

DOI: 10.1039/d0tc03430d

rsc.li/materials-c

Metal–orgainc frameworks (MOFs) are a class of hybrid inorganic/organic framework materials and have been widely used in smart sensing. Among them, MOF-based monochromatic luminescent sensors display a limited detecting accuracy due to their easily disturbed signal. Combining the merits of lanthanide (Ln) luminescence with a porous skeleton, Ln-functionalized dual/multiple-emitting metal–organic frameworks (MOFs) have exhibited potential applications in ratiometric luminescence sensing with high accuracy, antijamming, sensitivity, and selectivity. Through rational design or post-modification, MOFs can be endowed with intrinsic emissions from Ln ions, ligands, or other luminescent materials and served as advanced detection materials for a wide variety of analytes *via* the linear variation of the ratio of luminescence intensities. Herein, we have summarized the recent progress of Ln-functionalized MOF-based ratiometric probes in sensing analytes in organic solvents, aqueous systems, and gas phase as well as in detecting temperature and pH. According to the possible origin of emissions, three strategies, including embedding additional luminescent species, modulating "antenna effect", and mixed-Ln-based MOFs, are put forward for the construction of dual-emitting materials with high sensing performance.

1. Introduction

Metal–organic frameworks (MOFs), as porous and crystalline materials, are constructed by organic ligands and metal ions or clusters.[1] With abundant and adjustable structures and properties,[2,3] MOFs have exhibited potential applications in many fields, such as catalysis,[4,5] gas absorption and separation,[6,7]

College of Chemistry and Materials Science, and Guangdong Provincial Key Laboratory of Functional Supramolecular Coordination Materials and Applications, Jinan University, Guangzhou 510632, P. R. China. E-mail: danli@jnu.edu.cn

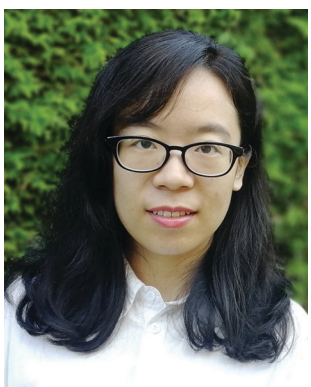

Yifang Zhao

Yifang Zhao received her BSc degree from Xiamen University in 2012 and PhD degree from Peking University in 2017. Currently, she is working with Professor Dan Li as a post-doctoral fellow at Jinan University. Her research interest includes the fabrication of porous photoluminescent materials, their sensing application, and the host–guest interaction within the confined space.

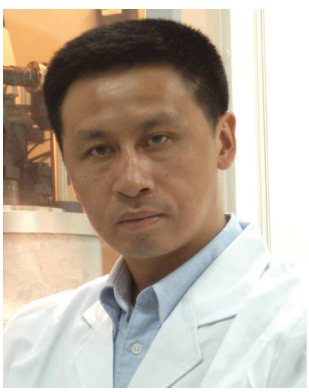

Dan Li

Dan Li received his BSc from Sun Yat-Sen University in 1984 and then worked at Shantou University. He pursued his PhD at the University of Hong Kong with Professor Chi-Ming Che during 1988–1993. Then he returned to Shantou University and became a professor in 2001. He moved to Jinan University in Guangzhou in 2016. He is a recipient of the National Science Fund for Distinguished Young Scholars of China in 2008 and a Fellow of the Royal Society of Chemistry (FRSC) in 2014. His research interest includes the design and fabrication of supramolecular coordination assemblies and their functions including photoluminescence, porosity and chirality.

and drug delivery.[8] In the area of smart sensing, MOFs have emerged as promising candidates over other materials, including metal complexes,[9] carbon nanotubes[10] and polymers,[11] because of their advantages below. With plentiful designable ligands or accessible metal sites,[12] MOFs can distinguish an analyte from interferences *via* the host–guest interactions with functional groups. The regular channels and the high surface area of MOFs can pre-concentrate the analyte within its confined spaces to further enhance the detection sensitivity.[13] Besides, the controllable pore size, shape, and surface character endow them with size and screen properties by matching well with the size of guests[14] and further increase the sensing selectivity. The crystallinity of MOFs promotes a thorough study of the detection mechanism using many techniques, like X-ray diffraction.[15,16] The explored regularities are beneficial for the design of specific sensors with improving sensing performance and property prediction. Moreover, the luminescence of MOFs originates from the metal ion, the ligand, and the guest, which allows exploiting the ratiometric sensors *via* constructing multi-emission materials.[17,18] Based on these merits, MOF-based luminescent sensors have been largely developed in the detection of ions,[19–21] explosives,[22] temperature,[23,24] volatile organic compounds (VOCs),[25] biomolecules,[26,27] and so on.[28,29]

With large Stokes' shifts, high colour purity, sharp and characteristic emission,[30] lanthanide-based optical materials[31] have been extensively used in optical devices,[32,33] optical storage and communication,[34] sensing[35,36] and bio-imaging.[37] Among them, the Ln-functionalized MOFs have attracted great interests in sensing,[38,39] because of their tunable luminescence properties and abundant energy transfer processes. Through the interaction between metals/ligands with a specific guest, the emission of Ln-based MOFs can be modulated and the obvious variation of luminescence colour allows the visual detection by naked eyes under UV light.[40] Until now, a majority of Ln-MOFs are monochromatic and applied as turn-on or turn-off probes in detecting ions,[41] VOCs,[42] biomarkers[43–46] *etc.*[47] However, the single emissive intensity is easily disturbed by the non-analyte factors, such as background luminescence and instrumental error, that influence the detection accuracy. This problem can be effectively solved by the construction of dual/multi-emission MOFs by introducing an extra emission source as a reference. The obtained materials can act as self-calibration probes if the ratio of two signals changes linearly with the concentration of the analytes. This kind of ratiometric materials has demonstrated higher and more exact sensing results than the mono-emission ones.[48,49]

In this review, we focus on the research studies of ratiometric Ln-functionalized MOF sensors in recent five years. Based on the origin of emission, three types of dual-emitting Ln-functionalized MOFs are put forward, including emission from Ln^{3+} and guest materials, emission from mixed Ln ions, and emission from Ln ions and ligands. Three construction strategies are used to build dichromatic MOFs, which are embedding additional luminescent species, modulating the "antenna effect" and mixed-Ln-based MOFs. Through these methods, a variety of Ln-functionalized MOF-based ratiometric sensors have been widely constructed and utilized in sensing analytes in an organic solvent, an aqueous system, gas phase as well as temperature and pH detection.

2. Luminescence properties and detection mechanisms

The rare earth series contains scandium (Sc), yttrium (Y) and lanthanides (lanthanum to lutetium, La–Lu). Due to the abundant electron transition levels, tunable coordination states, and large atomic magnetic moment, rare earth-based materials have been extensively pursued as optical, electrical, magnetic and multiple functional materials.[50–52] Therefore, rare earth metals have become one of the major strategic resources for many countries. In the optical field, with high quantum yields, long luminescence lifetimes, bright and sharp emission signals, lanthanide-based photonic materials have been largely developed in tunable lasers,[53] light-emitting diodes (LEDs),[54] sensing,[36] bio-imaging,[55] optical storage and communication.[56]

2.1 Luminescence of lanthanide ions

Generally, lanthanide ions are trivalent (except Eu^{2+} and Ce^{4+}) with a ground-state electronic configuration of $[Xe]4f^n$ (n = 0–14), which can generate a rich variety of electronic levels and translations.[57] Three kinds of electronic transitions may occur in Ln ions: 4f–4f transition, 4f–5d transition and charge-transfer transition. Among them, both the 4f–5d transition and charge transfer are broad, Laporte-allowed transitions and much dependent on the coordination surroundings of metal ions. However, these transitions usually appear at high energies in the UV range,[30,58] which is not beneficial for on-site sensing by naked eyes and are, thus, not discussed here. The 4f–4f transitions are Laporte-forbidden. The term "forbidden" can be explained as an allowed transition with low possibility, as the selection rules are derived based on several hypotheses and are hardly completely fulfilled in reality.[59] Due to the shielding effect of large radial subshells $5s^25p^6$, the Ln ions, except Ce^{3+}, exhibit sharp, narrow and unique emission spectra through 4f–4f transition as the 4f orbitals are hardly influenced by the crystal field effect. Ce^{3+} shows a broadband emission arising from allowed f–d transitions.[60] Eu^{3+}, Tb^{3+}, Sm^{3+} and Tm^{3+} emit the characterized red, green, orange and blue light in the visible region, respectively. Yb^{3+}, Nd^{3+} and Er^{3+} show near-infrared emissions. With a large energy gap, Gd^{3+} emits ultraviolet light and is hard to be sensitized by a regular ligand.[61] Among these lanthanide ions, Eu^{3+} and Tb^{3+} are most widely explored as response signals in MOF-based probes due to their bright emissions and detectable intensity changes in real applications. As shown in Fig. 1, Eu^{3+} emits red light with the main emission bands at around 590, 614, 651 and 697 nm, which can be assigned to the $^5D_0 \rightarrow {}^7F_n$ (n = 1–4), respectively. And emission bands of Tb^{3+} are around 488, 546, 588, and 621 nm, owning to the $^5D_4 \rightarrow {}^7F_n$ (n = 6–3) of Tb^{3+}.[62] Besides, other Ln^{3+} ions, like Ce^{3+}, Gd^{3+} and Dy^{3+}, are usually applied in fabricating mixed-Ln MOFs with multiple emissions, which contain the strong signal of Eu^{3+}/Tb^{3+}.[49,63,64]

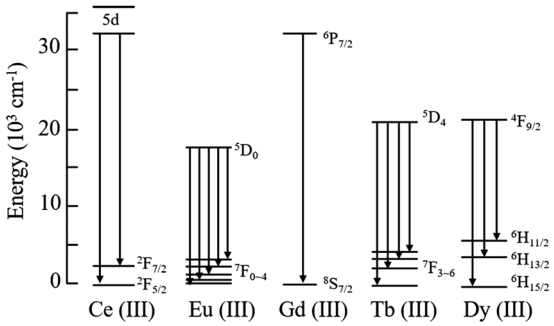

Fig. 1 Partial energy diagrams of the related lanthanide(III) ions in Ln-functionalized MOFs.

2.2 Antenna effect (process of sensitization)

In principle, it is hard to directly photo-excite Ln ions with high luminescence because of their narrow absorption cross section with limited absorption efficiency. This problem can be solved by the indirect excitation of Ln^{3+} by its coordinated antenna ligand, called as the "antenna effect".[65,66] Generally, an organic molecule can be motivated from the ground state (S_0) to the first excited singlet state (S_1) after absorbing excitation light with a suitable wavelength. Then the molecule in the excited state returns to its ground state through non-radiative or radiative way. The process of $S_1 \rightarrow T_1$ (triplet excited state) is termed as inter-system crossing (ISC). Among them, the radiative way leads to the luminescence emission of molecules, which is fluorescence ($S_1 \rightarrow S_0$) or phosphorescence ($T_1 \rightarrow S_0$). If the ligand has a good coordination ability with Ln^{3+} and the energy level of the T_1 state of the ligand matches well with the energy level of the Ln^{3+} ion, the energy in the T_1 state can funnel to the metal ion and result in its characteristic emission. Based on the Reinhold's empirical rule,[67] if the energy gap between S_1 and T_1 of the ligand is larger than 5000 cm^{-1}, the ligand can be used in sensitization. And the Ln ion can be effectively sensitized through "antenna effect" when the energy gap between the T_1 state of the ligand and the $^5D_0$ state of the Ln ion is larger than 3000 cm^{-1}.[68] For example, a common ligand, H_4BTEC (1,2,4,5-benzenetetracarboxylic acid) has the S_1 level at 39 841 cm^{-1} and the T_1 level at 20 790 cm^{-1}. As the energy difference between the T_1 state of H_4BTEC and the $^5D_0$ level of Eu^{3+} is 3290 cm^{-1}, H_4BTEC is an efficient sensitizer for Eu^{3+}.[43]

There are two types of Ln-functionalized MOFs, noted as Ln-MOFs and Ln@MOFs. In a Ln-MOF system, the Ln^{3+} ion acts as a metal node of MOFs and can be sensitized by the ligand through coordination bonds. Using the ion exchange method, Ln^{3+} can be loaded into the channel of the MOF matrix to form a Ln@MOF composite and emits the characteristic light *via* the weak interaction with the skeleton. Combined with the virtues of MOFs and "antenna effect" of the ligand, the Ln-functionalized MOFs have been widely developed in sensing due to the advantages below. The photoluminescence of lanthanides is usually weak because of self-quenching and the non-radiative decay by high energy vibrations of the coordinated solvents. By getting embedded into the rigid skeleton of MOFs, the emission and quantum yield of Ln^{3+} in Ln-based MOFs increases many-fold compared with the isolated one. Besides, with the large Stokes shift, the emissive properties of Ln^{3+} can be easily distinguished from the ligand-centred or guest-centred luminescence. The strong visible luminescence colour changes bring MOFs with the benefits for the real-time detection by naked eyes. In addition, the antenna effect is sensitive to the coordination environment of the Ln^{3+} ion. The guest–metal/ligand interaction can affect the sensitization process and further influence the luminescence property of Ln-modified materials. These merits endow Ln-contained MOFs the potential to probe the analyte with high detection performance.

2.3 Detection mechanisms

In a dual-emitting system with a variable Ln^{3+} emission as the sensing signal, the target molecule can be probed through the mechanisms below. Taking a Eu-MOF as an example, based on the sensitization process shown in Fig. 2, the luminescence property of the Eu^{3+} ion can be adjusted by the guest through three ways: blocking excitation light, regulating energy transfer processes and quenching emission. (1) If the absorption spectrum of the analyte overlaps with the excited light, a competitive light absorption occurs between the MOF and the analyte. The weakened light absorption ability of the ligand results in the quenching of Ln emission. (2) The sensitizing efficiency depends on the process of ET (energy transfer) and BET (back energy transfer). The factors, influencing these two processes, can further modulate the material's emission and be applied in designing sensors for specific guests. Through the ligand–guest interaction, the energy may partly transfer from the ligand to the analyte, which results in the receded ET and declined emission intensity of Eu^{3+}. For example, in a Eu^{3+}@JXNU-4 system, a fluorescence resonance energy transfer could occur from the ligand 4,4′-biphenyldicarboxylate to the guest 1-hydroxypyrene (1-HP) due to the overlapped excitation spectrum of 1-HP with the emission of the ligand. Therefore, the sensitizing efficiency was reduced and the emission of Eu^{3+} was quenched.[69] Besides, the ligand, H_2FDC (9-fluorenone-2,7-dicarboxylic acid) with a low T_1 energy level can

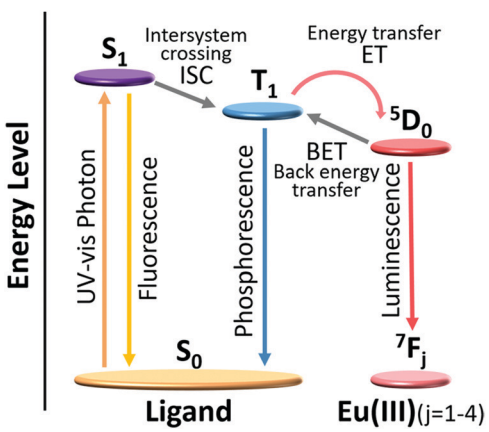

Fig. 2 Simplified Jablonski diagram of the "antenna effect" of Eu^{3+}.

hardly motivate Eu^{3+} and the obtained Eu-FDC is only a mono-emission material at room temperature. By lowering the temperature, the BET from the Eu^{3+} ion to the ligand is inhibited and the Ln-MOF exhibits dual-emitting property. This temperature-dependent luminescence performance makes this MOF a ratiometric thermometer.[70] In addition, the pH-induced tiny changes of the coordination states of Eu^{3+}, like the bond length, may also influence the ET process within MOFs, which was utilized in detecting acidic molecules, like acidic amino acids.[16,71] (3) Through the coordination interaction with the guest molecule, the emission of Eu^{3+} can be dissipated *via* the nonradiative decay by high energy vibrations, like O–H, C–H, N–H. In this regard, H_2O is a good quencher for Eu-MOF[72] and some Eu-MOFs have been explored to trace water in organic solvents[73–75] or medicine.[76]

Besides, the emission of Ln^{3+} can be introduced as a reference signal and the constructed MOFs can be applied as ratiometric sensors *via* a variational emissive ligand or guest. For instance, with a broad absorption at 260 nm and 360 nm, Cr(VI) can quench the emission of carbon dots (CDs) by absorbing the excitation and emission light. However, the luminescence property of the Eu-MOF remains unchanged. Combined with the reference signal of the Eu-MOF and its confined space for pre-concentration, the prepared composite could detect Cr(VI) as a self-calibrating probe with high performance.[77]

3. Constructive strategies for ratiometric Ln-functionalized MOF sensors

Based on the origin of luminescence, there are three classes of dual-emission Ln-contained MOFs: (1) emission from Ln^{3+} and another materials; (2) emission from the Eu/Tb ion and the ligand; (3) emission from mixed-Ln ions.[47] Due to the different nature of illuminant centres, the Ln-functionalized MOFs can detect species as the self-calibration probes through the different variation trends of signals. Three strategies to obtain dual-emission materials are summarized, including embedding additional luminescence species, modulating "antenna effect", and mixed-Ln-based MOFs (Fig. 3).

3.1 Embedding additional luminescence species

Due to the high surface area, regular channels and abundant interaction sites, MOFs are potential platforms to encapsulate the luminescent species in their channels or on their surface to build dual-emitting materials. By one-pot synthesis or post-modification, the illuminant guests are highly dispersed in the rigid skeleton of MOFs and their emission is stronger than the isolated one. An organic dye molecule is a kind of luminous material, which is widely applied as a colourant in daily life. Due to the plenty choices of the organic luminophore, the obtained dye@MOF system was largely explored in white LEDs,[78] nonlinear optical materials,[79] sensors[80–83] and so on.[84] The dye@MOF can be prepared through ion exchange with the counterions or covalently grafted by immersing the activated

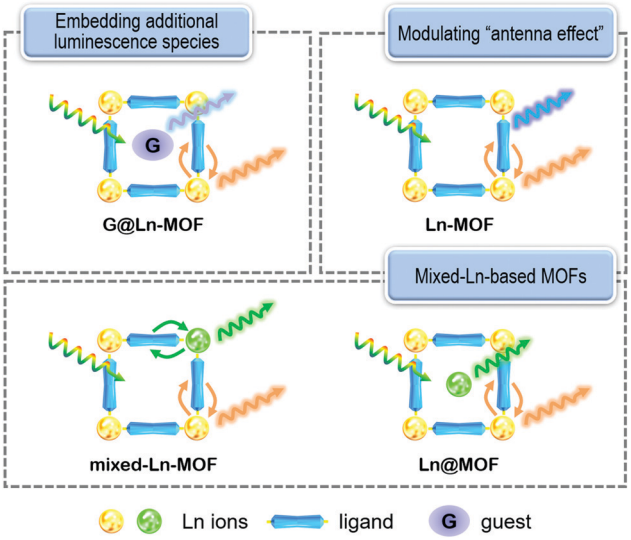

Fig. 3 Schematic representation of the three strategies to build dual-center emission Ln-MOFs reported so far.

MOFs into the solution of the dye for a certain time.[85] Through this process, the 1-HP fluorophore was incorporated into CoTb-DPA (DPA: dipicolinic acid) and the fabricated 1-HP@CoTb-DPA was applied in the detection of the pH value in the range of 0.3–5.0 even in human gastric juices as a ratiometric sensor.[83]

With tunable photoluminescence (PL), high chemical stability and low toxicity, CDs (carbon dots) have gained much attention as potential probes. CDs were usually synthesized *via* hydrothermal reactions[86] and introduced into the channel of MOFs during their formation.[87] For example, the synthesized CDs were added into an ethanol solution containing $Eu(NO_3)_3$ and DPA (2,6-pyridinedicarboxylic acid). Under a solvothermal condition for three days, a ball-flower-like CDs@Eu-DPA nanocomposite was fabricated. The dual emissions of the hybrid material originated from the Eu-DPA MOF and encapsulated CDs and the hybrid can detect Cu^{2+} as a self-calibration sensor with the LOD of 26.3 nM.[87]

In addition, fluorescein-labeled single-stranded DNA (*ss*DNA) has also been utilized as a fluorescent guest to couple within the MOF by adding the activated MOFs in the solution of *ss*DNA and stirred for several hours.[88] This kind of composite was employed in the detection of metal ions[89] or the target nucleic acid.[90] Furthermore, as a thermal-sensitive fluorescent material, Zn_2GeO_4:Mn^{2+} was constructed hydrothermally and immobilized with a Eu-BTC MOF (BTC = 1,3,5-benzenetricarboxylic acid) during MOF formation to build a self-calibrated sensor. The complex gave both red (Eu^{3+}) and green (Mn^{2+}) emissions, and exhibited the ratiometric thermal-sensing properties in the physiological temperature range (25–45 °C), with the S_m of 4.1% $°C^{-1}$.[91]

3.2 Modulating "antenna effect"

Most of the reported Ln-MOFs are monochromatic and exhibit an emission from a Ln ion or an organic ligand. As "antenna effect" is very sensitive to the coordination environment, the

incomplete energy transfer by modulating "antenna effect" through rational ligand design or regulating the external conditions will lead to dual-emitting materials with the emission from both Ln^{3+} and the ligand.

Due to the electron deficient property, boric acid was used to modulate the energy levels of a ligand and to influence the energy transfer efficiency from the ligand to the metal ion. Thus, boric acid-functionalized ligand, 5-boronoisophthalic acid (5-bop), was explored in the construction of dual-emitting Ln-MOFs with ratiometric sensing property.[92–95] Some ligands containing nitrogen, including tetrakis(4-carboxyphenyl)-pyrazine,[18] H_2BPDC (2,2′-bipyridine-5,5′-dicarboxylic acid),[65] and isonicotinic acid N-oxide (HINO),[66] were also used for constructing dual-emitting sensors for specific analytes. In addition, the mixed-ligand strategy was adopted for preparing self-calibrating probes.[74,76] For example, a novel Eu-MOF was constructed by the mixed ligands of dipicolinic acid (DPA) and 2-aminophthalic acid (PTA-NH_2), which owned the characteristic emission of PTA-NH_2 and Eu^{3+}. The dual-emitting MOF showed an ultra-sensitive property to water in real solid pharmaceuticals with rapid response (20 s) and long-term stability (30 days).[76] Furthermore, 4f–3d bichromatic materials[41,96–101] were synthesized to explore their ratiometric sensing properties. A dual-emission UiO-66 (Zr&Eu) was prepared from partly replaced Zr by Eu ions through one-pot synthesis. The MOF-based thin film was further obtained by depositing UiO-66 (Zr&Eu) in the polyvinylidene fluoride (PVDF), which could be used in the detection of temperature in the range of 237–337 K with the sensitivity of 4.26% K^{-1} at 337 K.[102]

What's more, the ratiometric materials can be fabricated on the basis of the monochromatic MOF *via* the regulation of the external conditions, like temperature[70] and the pH value.[16,71] In 2016, Carlos's group synthesized a new MOF with Eu^{3+} and H_2FDC. The prepared MOF only possessed an emission of the ligand upon excitation with visible light (450 nm), because the energy difference between the T_1 state of H_2FDC and $^5D_0$ of Eu^{3+} (553 cm^{-1}) is not large enough to effectively sensitize Eu^{3+} at room temperature. However, lowering the temperature could efficiently inhibit the back energy transfer from the metal ion to the ligand and resulted in the strong emission from Eu^{3+}. With this temperature-adjusted emission property, the Eu-MOF was applied as a ratiometric luminescence thermometer in the range of 12–320 K with a relative thermal sensitivity of 2.7% K^{-1} at 170 K.[70] In addition, the emission of the Ln-MOF can also be modulated by the pH value.[16,71] Recently, with the help of 2-fluorobenzoic acid, our group prepared a novel Eu-MOF with discrete trinuclear Eu clusters and ligand H_2NDC, which exhibited a pH-regulated luminescence switching property in the pH range of 3.00 to 4.00. Based on the analysis of SC–SC transformation from pH 4.00 to 3.00, this specific property was presumably attributed to the increased bond lengths of Eu–O_{NDC}, which may hinder the energy transfer from the ligand to Eu^{3+} and quench the luminescence of Eu^{3+} by enhancing that of the ligand. With this intrinsic property, the Eu-MOF could detect 3-nitropropionic acid quantitatively with the LOD of 12.6 μM.[16]

3.3 Mixed-Ln-based MOFs

Due to the similar coordination characteristics and atomic radii, mixed-lanthanide MOFs, including the EuTb-functionalized MOF, the EuDy-MOF,[63] the EuCe-MOF,[49] and the EuGd-MOF,[103] can be easily prepared by one-pot synthesis or ion exchange. By doping two or more lanthanide ions at the same crystallographically equivalent positions, the MOFs were endowed with two emission sources from Ln^{3+} ions or ligands. Among them, EuTb-functionalized MOFs have been most largely used in the detection of temperature,[104–109] biomarkers[110–112] and so on.[40,75,113–115] This kind of MOF requires a ligand with a T_1 state energy level in the range of 22 000 to 27 000 cm^{-1}, which is higher than the main accepting levels of Eu^{3+} ($^5D_1$ 19 030 cm^{-1}) and Tb^{3+} ($^5D_4$ 20 500 cm^{-1}).[116] Eu^{3+} can be sensitized by both the ligand and Tb^{3+}. With organic ligand 5-(pyridin-4-yl)-isophthalate (PIA), a series of EuTb-PIA MOFs were constructed and they exhibited tunable emissions from red to green with an increasing doping amount of Eu^{3+} from 0 to 10%. Due to the temperature-dependent luminescence colours, this kind of material showed the potential as a ratiometric thermometer (Fig. 4).[116]

Similarly, a $Eu_{0.02}Dy_{0.18}$-MOF with three emission centers was fabricated with Eu^{3+}, Dy^{3+} and 5-(bis(4-carboxybenzyl)-amino)-isophthalic acid to employ them as dual-functional self-calibrated sensors for the detection of temperature and water in bioethanol.[63] Besides, Qian's group developed a MOF, ZJU-136-CeEu, showing emissions of Eu^{3+} and a ligand of 1,1′:4′,1″-terphenyl-2′,4,4″,5′-tetracarboxylic acid, to be a ratiometric fluorescent probe for detecting ascorbic acid (AA).[49] In the other example of a EuGd system, as the excited energy levels of Gd^{3+} are too high to be sensitized, the EuGd-MOF emits from the ligand and doping tiny amount of Eu^{3+}. For instance, Eu^{3+} can be effectively sensitized by the ligand 1,4-naphthalene dicarboxylic acid (H_2NDC), while Gd^{3+} is hard to be activated. By doping a certain content of Eu^{3+} in Gd-NDC, the MOF possessed both the emissions of Eu^{3+} and NDC^{2-} and their luminescence property could be easily tuned with different doping amounts of Eu^{3+}. This mixed-Ln MOF could detect

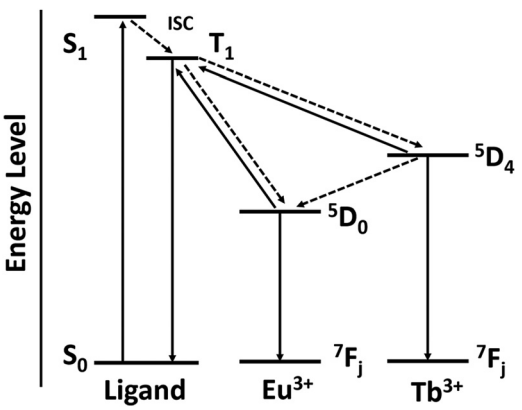

Fig. 4 Schematic representation of energy transfer processes in the luminescent EuTb-MOF.

temperature in the physiological range (20–60 °C) with a relative sensitivity of 5.19% $°C^{-1}$.[103]

4. Ln-Functionalized MOF ratiometric sensors for various applications

With multiple emissive centers, Ln-contained MOFs are rapidly growing for quantifying the analyte ratiometrically in recent years. In this section, the latest development of Ln-functionalized MOFs for detecting various species, including water, ions, biomolecules, *etc.*, will be elaborated to demonstrate their applications in different areas. Based on the detection phase systems, the Ln-MOFs with accessible metal coordination sites for water molecules can trace water in organic solvents. The composites without the water–disturbance property are utilized in sensing the analytes in an aqueous system and gas phase. Besides, the MOFs have also exhibited the potential as self-calibrating thermometers or pH sensors, due to their temperature/pH-sensitive luminescence properties.

4.1 Water detection

The presence of trace water in organic chemicals or drugs can influence their daily uses and activities. Developing a facile and rapid tracing water method in solvents or drugs is important in chemical industry.[117] When water molecules coordinate with lanthanide ions, the nonradiative deactivations occur *via* the high-energy vibrations. The relative quenching degree depends on the concentration of involved chemical bonds.[72] Therefore, with the accessible site of the Ln ion, the Ln-MOF possesses the ability to trace water quantitatively in organic chemicals[73–75] or medicine.[76] Chi's group constructed CDs@Eu-MOF nanohybrids through the encapsulation of N,S-codoped CDs in the channels of the MOF, which contained the emission of Eu^{3+} and very weak photoluminescence of CDs. The obtained hybrid could detect the content of water in ethanol through the linearly changed ratio of I_{420}/I_{623} in the water content range of 0.05–4%, with the LOD of 0.03% (v/v%). The author speculated that, in the presence of water, CDs in the channels were released into the solution with enhanced emission and the luminescence of the Eu-MOF was quenched by O–H oscillators *via* the access of water molecules (Fig. 5).[73] In addition, a $Eu_{2.89}Tb_{97.11}$-MOF was prepared with mixed-Ln ions and the ligand hexakis(4-carboxylatophenoxy)cyclotriphosphazene. This demonstrated the ratiometric sensing property for trace water in CH_3CN rapidly, reversibly and sensitively (LOD of 0.04%). With the hydrophilic cavity and the contactable metal site, the emissions of Eu^{3+} and Tb^{3+} in MOFs were quenched within several seconds by H_2O, showing a linear relationship between the ratio of I_{543}/I_{615} and the content of water in CH_3CN in the range of 0% to 2.5%.[75]

Deuterium oxide (D_2O), an isotopically labeled water molecule, plays a significant role in chemical analysis and medicine. With the similar size and properties, monitoring the trace water contamination in D_2O is vital but really challenging. Compared with O–H, O–D is a low-frequency oscillator. When H_2O is replaced by D_2O, the emission of Ln^{3+} can be recovered due to the reduced vibronic deactivation pathway.[118] Thus, the water-responsive Ln-MOFs also displayed an ability to identify H_2O in D_2O or D_2O in H_2O. In 2017, through ion exchange, a series of mixed-Ln@PCN-22 was developed with tunable luminescence property. These materials could effectively detect H_2O in D_2O and other solvents, including acetone, ethanol and acetonitrile. Among them, Eu_1Tb_5@PCN-22 could quantify H_2O in D_2O in the range of 10–120 000 ppm with the limit down to 0.1% v/v. Furthermore, a series of EuTbGd@PCN-22 was constructed for eight-factor solvent fingerprinting to differentiate 18 solvents even by naked eyes based on the CIE coordinates and relative emission intensities of these materials (Fig. 6).[119] Recently, a bimetallic uranyl/Eu-MOF $(TEA)_3[(UO_2)_6Eu(H_2O)_4(PPA)_6]$ (PPA: phosphonoacetic acid, TEA: tetraethylammonium cation) was obtained hydrothermally with the characteristic emissions of UO_2^{2+} and Eu^{3+}. This MOF could detect D_2O in H_2O within a full range through an increased Eu^{3+} signal and unchanged emission of uranyl. The specific response is explained by the more labile and more coordinated water molecules with Eu^{3+} than UO_2^{2+}, which could effectively influence the emission of Eu^{3+} through H_2O–D_2O exchange. Besides, the sufficient ET from UO_2^{2+} to Eu^{3+} impaired the enhanced emission of UO_2^{2+}. This bimetallic MOF could probe heavy water with the detection limit of 1%.[120]

In the Ln-MOFs with unapproachable metal sites, H_2O can be probed through the affected fluorescence of a ligand *via* the

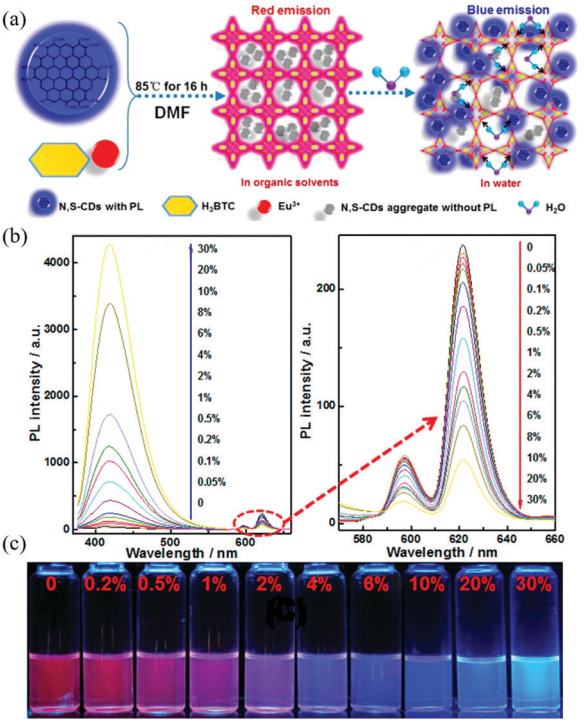

Fig. 5 (a) Scheme of synthesis and detection of water in the CDs@Eu-MOF. (b) PL spectra and (c) the related photos of the CDs@Eu-MOF in ethanol upon adding different contents of water under 365 nm excited light.[73] Reproduced from ref. 73 with permission from the American Chemistry Society, copyright 2016.

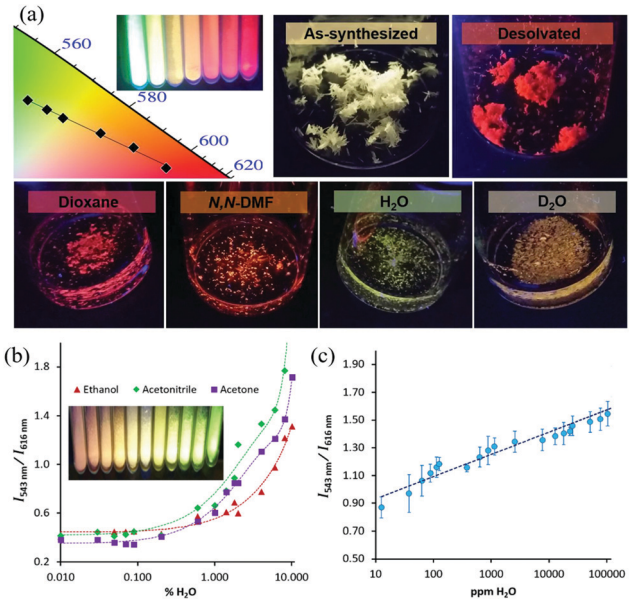

Fig. 6 (a) CIE coordinates of various Eu_xTb_y@PCM-22 compositions; photos of as-synthesized, desolvated Eu_1Tb_1@PCM-22 and the exposure of the same desolvated material to four different solvents (dioxane, DMF, H_2O, and D_2O). (b) Relative photoemission response ratio curves upon the addition of H_2O to activated Eu_1Tb_5@PCM-22 and (c) the linear curve of Eu_1Tb_5@PCM-22 for trace H_2O in D_2O. Error bars were obtained from three separate experiments.[119] Reproduced from ref. 119 with permission from Elsevier, copyright 2017.

ligand–guest interaction. In 2019, with the mixed-ligands 2-aminoterephthalic acid (atpt) and 1,10-phenanthroline (phen), a Eu-MOF was synthesized with the luminescence originating from Eu^{3+} and atpt. As a turn-on and self-calibrated sensor, this MOF could probe water in organic solvents (DMF, acetone, and ethanol) with the enhancing emission of atpt and the unchanged emission of Eu^{3+}. The detection limit is as low as 0.01%. The mechanism is attributed to the H_2O-reinforced intramolecular charge transfer (ICT) emission of atpt, while other solvents could not. The distinct emission change from red to blue of the Eu-MOF was favourable for visual detection by naked eyes with the LOD of 0.11% (v/v%). The MOF-based water analytical logic device and test paper were further developed for sensing water in solid pharmaceuticals rapidly (20 s) and sensitively (Fig. 7).[76]

4.2 Sensing in an aqueous system

With rigid skeletons and unreachable metal sites, some Ln-based MOFs have stable luminescence properties in an aqueous system, because the water molecule is impeded to access Ln^{3+} or the coordinated water has little effect on its emission. Without the disturbance of water, this kind of MOF exhibits an exact detection performance in sensing cations, anions, nitroaromatic compounds and biomolecules in an aqueous system. Metal ions play an important role in the environment and organisms and the abnormal level of metal ions in organisms may result in unhealthy or even disease in living bodies. Therefore, monitoring metal ions, like Fe^{3+},

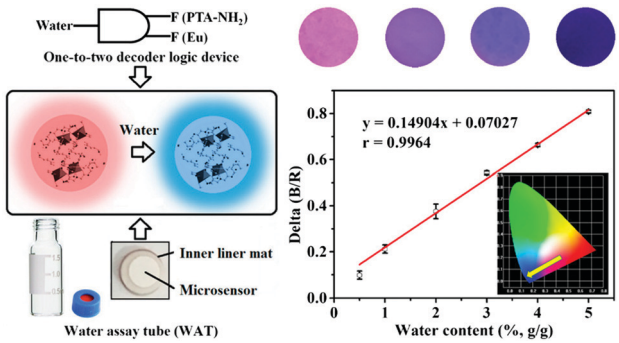

Fig. 7 Mixed-ligand Ln-MOF based logic device for the ratiometric detection of water in organic solvents and solid pharmaceuticals.[76] Reproduced from ref. 76 with permission from the American Chemistry Society, copyright 2020.

Cr^{3+}, and Hg^{2+}, in soil and water is really meaningful to the environment, human health and food safety and has attracted much attention in recent years.[121,122] In 2018, Zhao's group prepared a tri-emission EuTb-MOF with a flexible ligand, hexa-(4-carboxyl-phenoxy)-cyclotriphosphazene (CTP-COOH) and a MOF-based film with the help of polyvinyl alcohol (PVA). The constructed film could distinguish different metal ions through two-dimensional (2D) readout and the related decoded map was obtained for the fingerprint recognition of these metal ions. This ion-dependent response may be caused by the host–guest interaction, which modulates both the energy transfer from the ligand to Ln^{3+} and the energy assignation by affecting $Tb^{3+} \rightarrow Eu^{3+}$. Among these ions, the MOF-based film could detect Fe^{3+} within 10 s with the LOD of 3.86 μM. Besides, this PVA film could also recognize different VOCs in 2D readouts and detect vaporous styrene within 4 min with a quenching efficiency of 97% (Fig. 8).[107] In 2019, Eu^{3+}@CAU-11, a sulfone-functionalized MOF, was developed as a ratiometric probe of metal ions. The obtained material could distinguish Cu^{2+} and Fe^{3+} from others, through the changed ratio I_L/I_{Eu}. Fe^{3+} could influence the emissions of the composite in both water and *N*,*N*-dimethylformamide (DMF), while Cu^{2+} could only be realized in DMF, which might be caused by the competitive coordination between Eu^{3+} and Fe^{3+} or Cu^{2+}. On the basis of the specific response to these two ions, a logic gate could be designed for the distinction of these ions portably and clearly.[123]

Copper is a vital trace biological element that maintains the activities of some proteins.[124] However, the overtaking of the Cu^{2+} ion can result in its accumulation in organisms and cause some diseases. Thus, monitoring the content of Cu^{2+} in drinking water or body fluid can efficiently ensure the health of the human body. In 2018, a Eu/FITC-functionalized Fe_3O_4@ZIF-8 (FITC: fluorescein isothiocyanate) nanoprobe exhibited an effective sensing property for Cu^{2+} with a declining signal of Eu^{3+} and the unchanged emission of FITC. This material could detect the copper ion as a ratiometric probe with the detection limit of 0.1 nM, which is lower than the allowing amount of Cu^{2+} in drinking water as prescribed by EPA. And it could even be applied for Cu^{2+} imaging in real samples and live cells.[125] Besides, by coupling with CDs, a ball-flower-like CDs@Eu-DPA

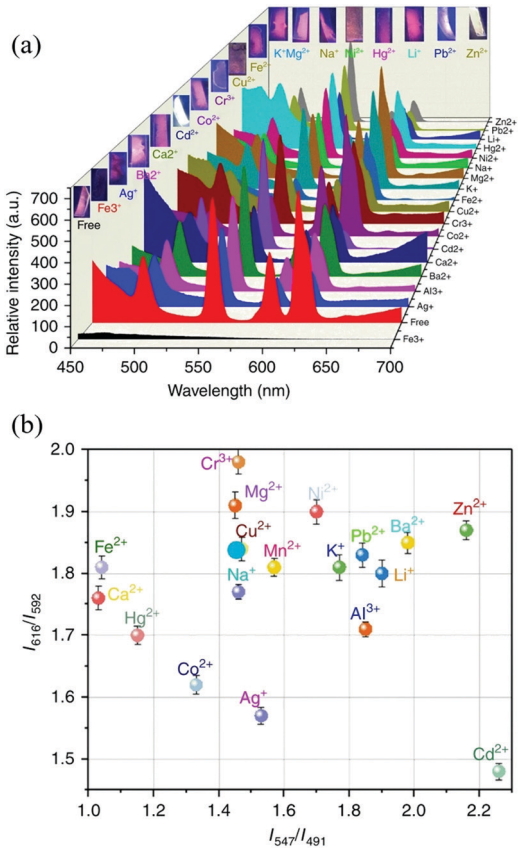

Fig. 8 Metal ion decoding and Fe^{3+} sensing of the $Eu_{0.47}Tb_{0.53}$-CTP-COOH PVA film in an aqueous solution.[107] Reproduced from ref. 107 with permission from the nature, copyright 2018.

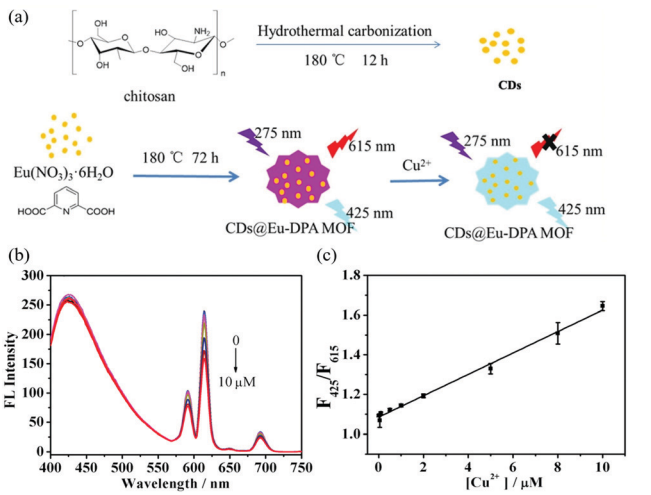

Fig. 9 (a) Scheme of the synthetic route and Cu^{2+} detection of CDs@Eu-DPA. (b) Fluorescence spectra and (c) linear calibration plot of CDs@Eu-DPA nanocomposites in the detection of Cu^{2+}.[87] Reproduced from ref. 87 with permission from Elsevier, copyright 2017.

composite was constructed by one-pot synthesis for the detection of Cu^{2+} among other ions. The author deduced that the strong coordination ability of Cu^{2+} with the nitrogen atom of DPA inhibited the energy transfer from the ligand to the metal and resulted in the emission quenching of Eu^{3+}. This composite could detect Cu^{2+} in the range of 50 nM–10 μM with the LOD of 26.3 nM as a self-calibration sensor (Fig. 9).[87] In 2017, Eu^{3+} and FAM-labeled ssDNA were introduced into Bio-MOF-1 through ion exchange. The obtained platform showed a good selectivity for Cu^{2+} amongst other ions with the LOD of 0.14 μM, by the fading of FAM and the increasing signal of Eu^{3+} ions. After detecting the Cu^{2+} ion, the composite was applied in sensing S^{2-} subsequently, due to the affinity between Cu^{2+} and S^{2-}.[89]

To monitor the contents of Hg(II) and Cr(VI), as fatal toxicants, in drinking water and daily food is really meaningful to global health.[126] In 2016, Yan's group prepared Eu^{3+}/CDs@MOF-253 by encapsulating highly fluorescent species Eu^{3+} and CDs into MOF-253, which had excellent luminescence properties and stability. The obtained material could distinguish Hg^{2+} from other ions through the linearly increasing ratio of I_{Eu}/I_{CDs} with the concentration of Hg^{2+} in the range of 0.065–150 μM. The author attributed it to the interaction between Hg^{2+} and the functional groups of CDs, which could modulate the energy transfer processes within CDs and thus quench their emission, while the luminescence properties of Eu^{3+} was merely unaffected. The hybrid material could detect Hg^{2+} as a ratiometric and colormetric sensor with the LOD of 13 ppb and even remove it from environmental samples (Fig. 10).[127] In 2019, a CDs@Eu-BTC MOF was developed by encapsulating N,Co-co-doped CDs in the Eu-MOF and demonstrated high detection activities toward Cr(VI). With the addition of Cr(VI), the emission of CDs centred at 467 nm was quenched and that of the Eu-MOF was retained. The possible mechanism was ascribed to the inner filter effect of Cr(VI), which could absorb both the excitation and the emission light of CDs and resulted in its quenching. This material could detect Cr(VI) with the LOD of 0.21 μM and even in the real samples, like Yellow River.[77]

Ln-functionalized MOFs were also explored in the detection of anions. In 2017, a Eu-MOF, formed by 5-bop, exhibited two emissive peaks at 320–500 nm and 590–750 nm upon excitation at 275 nm. The synthesized MOF could distinguish F^- from other anions with enhanced emission around 366 nm and the weakened one at 625 nm. The detection mechanism is attributed to the strong interaction between boron and fluoride, which could form the $-BF_3$ group through OH^-/F^- exchange, weaken the intersystem crossing efficiency and thus affect the luminescence of the MOF (Fig. 11).[92] Through post-modification, Eu^{3+} ions were anchored on the amino sites of MIL-125(Ti) to build the dual-emitting composite Eu^{3+}@MIL-125 for rationmetric recognition of anions. With the anion-dependent I_L/I_{Eu} and quantum yield, the orthogonal pattern readout could be obtained for distinguishing different anions, including SO_3^{2-}, PO_4^{3-}, ClO^-, CO_3^{2-}, *etc.*[128] In addition, a heterobimetallic MOF, Eu/Pt-MOF, was constructed with H_2BPDC, in which the Pt(II) ions were anchored by N atoms of the ligand. This MOF exhibited emissions of both Eu^{3+} and $BPDC^{2-}$ and could detect CO_3^{2-} amongst other anions with a LOD of 0.021 μM self-calibratingly. The increasing emission of Eu^{3+} was due to the coordination of carbonate groups with Eu

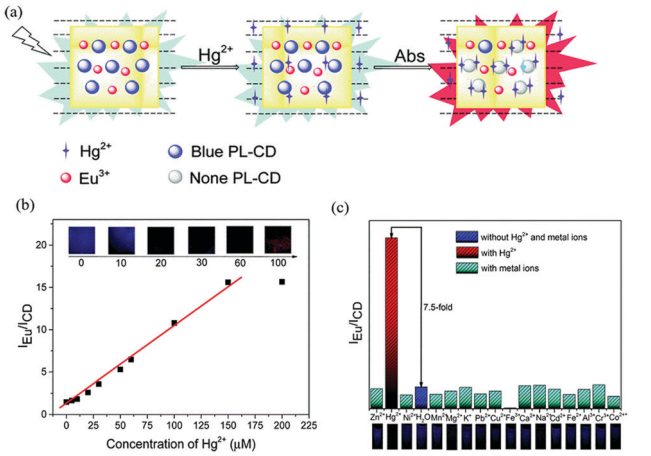

Fig. 10 (a) Schematic of the Hg^{2+} detection mechanism using Eu^{3+}/CDs@MOF-253. (b) Linear relationship between I_{Eu}/I_{CD} and C_{Hg}. (c) I_{Eu}/I_{CD} of Eu^{3+}/CDs@MOF-253 in aqueous solutions with different metal ions.[127] Reproduced from ref. 127 with permission from the Royal Society of Chemistry, copyright 2016.

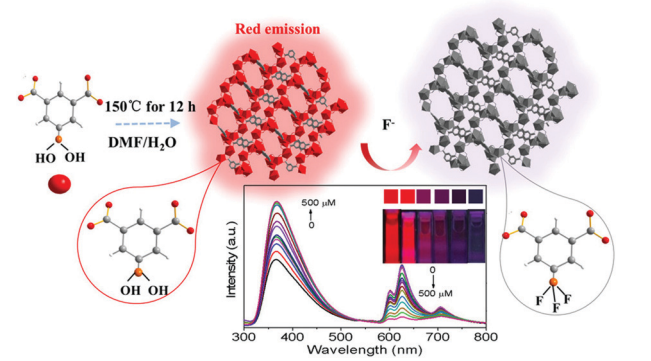

Fig. 11 Boric acid functional Ln-MOF for the ratiometric detection of F^-.[92] Reproduced from ref. 92 with permission from the American Chemistry Society, copyright 2017.

clusters, in which the electronegative C–O bond could improve the sensitized efficiency.[129]

Picric acid (PA) is an explosive material. In 2018, a rod-like nano dye@Eu(BTC) was prepared by linking the rhodamine-based dye (RBH) with the Eu-MOF, which could act as a dual-probe towards PA with a LOD of 10 μM, through ratiometric fluorescence and colorimetric sensing. The specific response was explained by the proton-induced structural conversion of the dye and the quenching effect of the nitrophenyl group in PA, which resulted in the increasing signal of the dye and fading one of Eu^{3+}.[81] Besides, with the ligands of *N*-methyl-2-pyrrolidone (NMP) and [1,1′:4′,1″-terphenyl]-2′,4,4″,5′-tetracarboxylic acid (H_4L), a series of isostructural Ln-MOFs were synthesized with tunable luminescent properties. Among them, the Tb-MOF and the $Tb_{0.01}Gd_{0.99}$-MOF exhibited the emissions of both Tb^{3+} and the ligand and could probe PA as a ratiometric sensor through the linearly changed I_{Tb}/I_L. The author deduced that the emissions of MOFs were quenched at different rates through photo-induced electron transfer (PET) and Förster resonance energy transfer (FRET). The detection limits were calculated to be 0.11 and 0.41 μM, respectively.[113]

Biosensing is a technique to monitor the biomolecules or biomarkers in the environment or organisms selectively, which plays a significant role in food safety, healthcare and diagnostics. With the designable structures and properties, MOF-based biosensors have been widely employed in sensing biomolecules, including amino acids,[68,71,98] ascorbic acid,[49,101] glucose,[93] dopamine,[94] and biomarkers, like DPA,[82,110,111,130] 1-HP,[69] *etc.*[131]

Amino acids are fundamental constituents of polypeptides and proteins in the development of living organisms.[132] Thus, sensing amino acids with high sensitivity and selectivity is really essential but very challenging. In 2019, with an aggregation induced-emission (AIE) ligand, tetrakis(4-carboxyphenyl)-pyrazine, a dual-emitting Eu-MOF was constructed and applied in monitoring the antenna effect and coordination induced emission (CIE) during its formation. The obtained Eu-MOF could detect Arg from other amino acids with the LOD of 15 nM self-referencingly. The detection mechanism is deduced to the formation of hydrogen bond interaction between the guanidinium group on arginine and the pyrazine core of the MOF, which restricted the rotation of the benzene ring of the ligand and enhanced its emission intensity. Therefore, with the addition of Arg, the blue emission of the Eu-MOF was enhanced and the red emission remained constant, acting as a reference (Fig. 12).[68] In 2019, our group prepared a Eu-MOF with H_2NDC, which possessed the pH-modulated luminescence switching properties. By lowering the pH value from 4 to 3, the emission of the Eu-MOF changed from red (Eu^{3+} dominated) to blue (NDC ligand dominated) gradually. Through the study of SC–SC transformation of this process, the mechanism of the switching property was attributed to the changed coordination environment

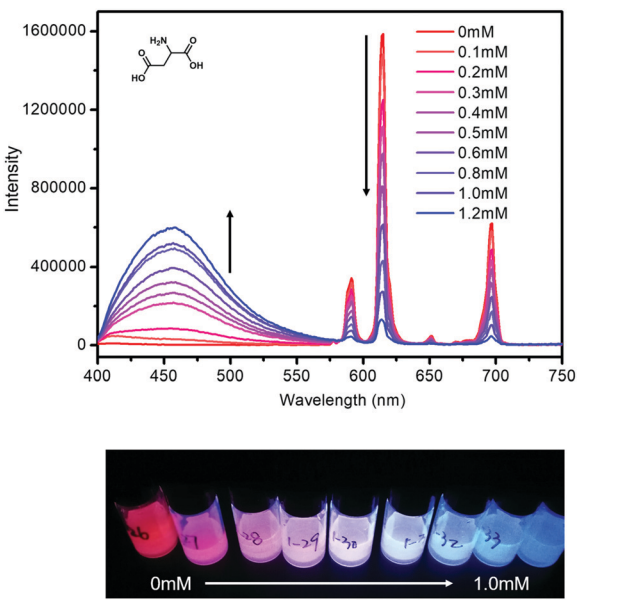

Fig. 12 Fluorescence of acidic amino acids detecting Eu-NDC and the corresponding photo under UV light.[71] Reproduced from ref. 71 with permission from the Royal Society of Chemistry, copyright 2019.

of Eu^{3+}, wherein the coordinated DMF molecule was replaced with the water molecule rapidly and the Eu–O bonds elongated slightly. Through these changes, the energy transfer from the ligand to Eu was weakened and thus the emission of Eu^{3+} was quenched with the enhancing luminescence of the ligand. Due to its specific pH-triggered luminescence switching property, the MOF could rapidly distinguish the acidic amino acid (aspartic acid and glutamic acid) from other amino acids, with LODs 21 μM and 22.4 μM, respectively (Fig. 12).[71]

As a main energy source and important matter in organisms, glucose is usually detected *via* sensing H_2O_2 instantly with glucose oxidase (GOx), because the GOx can oxidize glucose with the by-production of H_2O_2. For example, with 5-boronobenzene-1,3-dicarboxylic acid, a Eu-MOF was synthesized and emitted light centered at 354 nm and 623 nm upon excitation at 270 nm. The formed hydroxyl group through the nucleophile reaction between boric acid group and H_2O_2 could inhibit the intersystem crossing efficiency for Eu^{3+} sensitization. Therefore, this Eu-MOF could detect H_2O_2 irreversibly with the LOD of 0.0335 μM, with the enhancement of blue light and quenching of the red one. With the help of glucose oxidase (GOx), this MOF could also sense glucose with the detection limit of 0.0643 μM (Fig. 13).[93]

Biomarkers are indicators of diseases or toxin chemicals. The detection of a biomarker plays a significant role in diagnosis and prognosis in theranostics and assessment of chemical exposure and the environment. Anthrax is an acute infection caused by *Bacillus anthracis* spores and can damage the skin, lung and bowel of living bodies.[133] Dipicolinic acid (DPA) is the major component of *Bacillus anthracis* and is, thus, treated as a biomarker of anthrax.[134] In 2016, Eu/Tb@bio-MOF-1 was prepared by ion exchange, which exhibited the emissions of both Eu^{3+} and Tb^{3+}. This material could distinguish DPA from other aromatic ligands or amino acids through the emission variation from red to green. According to the result of luminescence decay dynamics, this unique colour change is attributed to the transformation of the energy transfer process in the presence of DPA. Due to the more coordination probability of DPA to Tb^{3+} than Eu^{3+}, PDA may coordinate with Tb^{3+} by replacing the coordinated solvent and even influence the energy transfer of Tb to Eu. Thus, DPA could be detected with a LOD of 34 nM even in the undiluted serum samples.[97]

Similarly, a bimetallic Eu/Tb-BTC nanosensor was constructed through rapid and direct precipitation, which could probe DPA with the emission colour changing from red-orange to yellow-green. With the modulated energy transfer processes by DPA along with the competition absorption of excitation light between DPA and the ligand, the red emission of the MOF was declined and the green emission was enhanced. The detection limit of Eu/Tb-BTC to PDA was as low as 4.55 nM, which is much lower than the infection dose of human (60 μM).[135] Furthermore, the Eu/Tb-BTC-based test strips were prepared to detect DPA in human serum samples by naked eyes (Fig. 14).[111] Besides, Yu's group covalently grafted a rhodamine-like dye to Eu(BTC) by the post-modification of the colorimetric and ratiometric luminescence response to DPA. The detection mechanism was explained by the photon-promoted structural transformation of rhodamine and modulated energy transfer from the MOF to the electron-pulling pyridine ring of DPA, which could enhance the signal of the dye molecule and decrease that of Eu^{3+}.[82]

As an important industrial compound, toluene diisocyanate (TDI) has been widely used in the automotive industry and building insulation.[136] However, due to its irritation to the mucous membranes of eyes and respiratory tract, the uptake of the residue TDI can cause some health problems like asthma. Thus, detecting diaminotoluene (TDA), the metabolite and biomarker of TDI, can effectively evaluate the exposure to TDI.[137] In 2018, dual-emitting Eu^{3+}/CDs@MIL-53 was found to recognize the TDA as a ratiometric fluorescent probe with the sensing limit of 6.8 μg mL^{-1}. The mechanism was attributed to the dynamic quenching process through non-radiative deactivation, as the reduction of lifetime is proportional to the TDA concentration.[131]

The illuminant 1-HP, the main biomarker and metabolite of PAHs, is usually treated as an indicator for the exposure to PAH mixtures and was detected by a mono-emitting MOF as a self-calibration sensor. *Via* ion exchange, Eu^{3+} was incorporated within JXNU-4 and sensitized by the ligand effectively. The Eu^{3+}@JXNU-4 could sense 1-HP with the increasing emissive intensity of 1-HP at 502 nm and decreasing emission of Eu^{3+} at 616 nm. The detection mechanism was ascribed to the

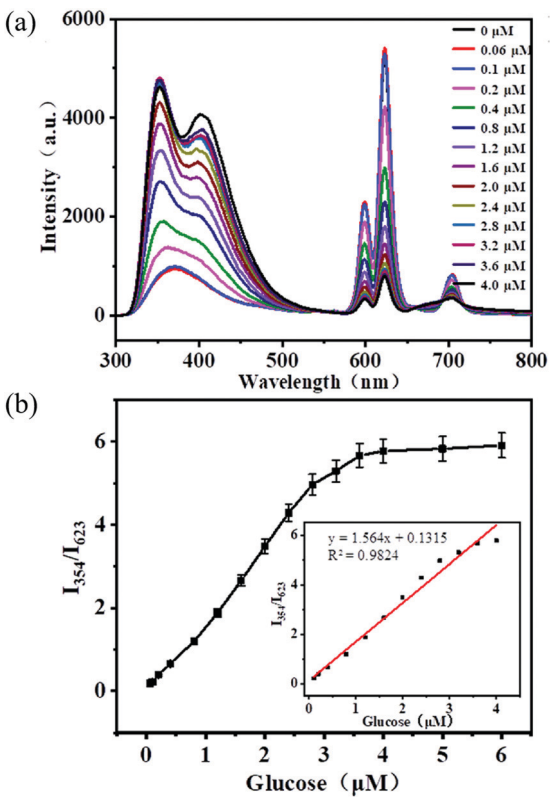

Fig. 13 (a) Fluorescence spectra of the sensing platform at different concentrations of glucose. (b) Plot of the intensity ratio of I_{354}/I_{623} vs glucose concentration under UV irradiation.[93] Reproduced from ref. 93 with permission from Elsevier, copyright 2019.

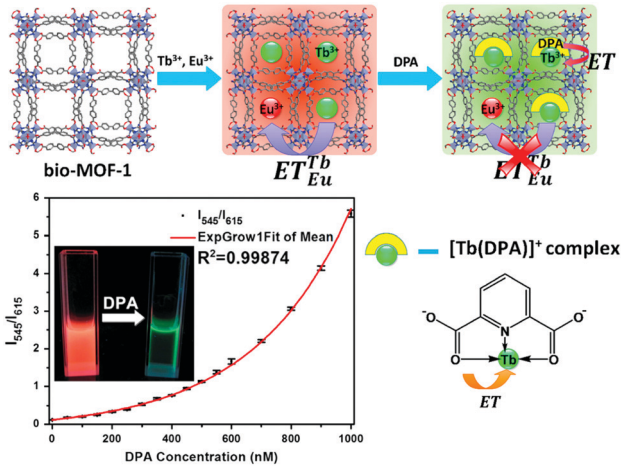

Fig. 14 Synthesis strategy of Tb/Eu@bio-MOF-1 and its calibration plot and schematic diagram for the detection of DPA.[110] Reproduced from ref. 110 with permission from the Elsevier, copyright 2016.

fluorescence resonance energy transfer (FRET) from the ligand to 1-HP, which weakened the antenna effect on Eu^{3+} and quenched its emission.[69]

H_2S, a well-known toxic gas, is involved in some physiological processes in organisms. As the oxidized product of L-cysteine, the abnormal level of H_2S in the body has been demonstrated to be related with some diseases.[138] Thus, developing an effective sensor for H_2S in organisms is of great significance for disease diagnosis.[87,96,139] In 2018, a EuCu-MOF was built with 2,3-pyridinedicarboxylic acid (H_2pydc) and oxalic acid (ox), which exhibited the emissions of Eu^{3+} and $pydc^{2-}$. Due to its unsaturated electronic state ($3d^9$), Cu^{2+} in the MOF had an affinity to electrons and weakened the emission of Eu^{3+} *via* limiting the "antenna effect". With the addition of electron-donated guests, like H_2S, Cu^{2+} formed a strong binding to these molecules. The quenching effect of Cu^{2+} was inhibited and the emission of Eu^{3+} was enhanced up to 9-fold. Therefore, the CuEu-MOF could detect H_2S with the LOD of 130 nM (Fig. 15).[96] Based on the similar mechanism, a CDs@ZIF-8@GMP/Tb (GMP: guanosine monophosphate) composite was prepared with GMP as a bridge ligand to combine ZIF-8 with GMP/Tb coordination polymers, which was employed as a H_2S sensor *via* Cu^{2+}-mediated fluorescence. By purging the quenching effect of Cu^{2+} by H_2S, the hybrid material could detect H_2S with a detection limit of 150 nM for spectroscopy and 3 μM for naked eyes even in serum samples and distinguish it from other thiols and biological species.[140]

4.3 Gas detection

As a threat to human health, VOCs[114,141,142] are significant in influencing the air quality. In 2016, a 4d–4f Ag^+/Eu^{3+}@UiO-66-COOH nanocrystal was developed through ion exchange and emitted the characteristic light of Eu^{3+} and the organic ligand. Its luminescence property could be governed by the incorporation of Ag^+ by altering the electronic structure and the energy transfer process. This material was demonstrated to be an

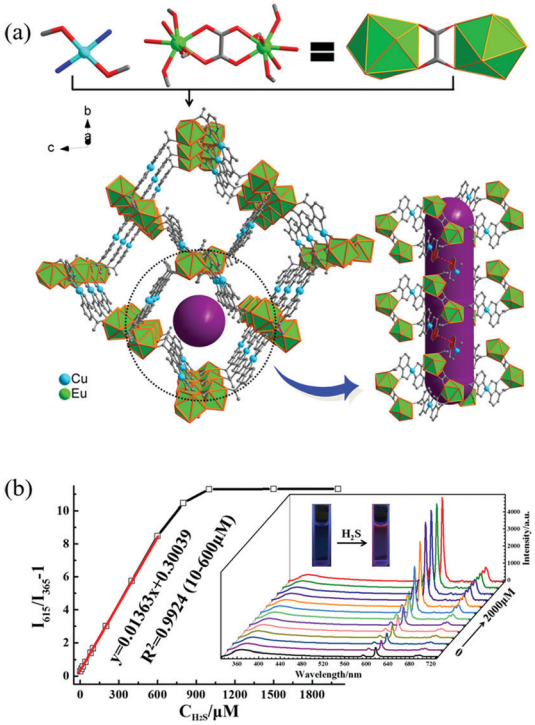

Fig. 15 (a) Crystal structure of the CuEu-MOF viewed along *a* crystallographic direction. (b) Concentration-dependent PL spectra of the CuEu-MOF in the H_2S solution.[96] Reproduced from ref. 96 with permission from the American Chemistry Society, copyright 2018.

outstanding nanoprobe for indoor formaldehyde (FA) with a LOD of 51 ppb. The author deduced that the interaction between FA and Ag^+ could inhibit Ag^+'s influence on the energy transfer process in this material, and thus the emission of Eu^{3+} was increased accompanied with the decreasing of the ligand's emission (Fig. 16).[141] In 2017, Yan's group constructed dual-emitting Eu-ZnO@UiO by incorporating the Eu^{3+}-loaded ZnO within the UiO-MOF. With a large surface area for pre-concentrating, the obtained heterostructure exhibited response to the volatile aldehyde gases, including FA, AA (acetaldehyde), and ACA (acraldehyde), with LODs of 42 ppb, 58 ppb and 66 ppb, respectively. The mechanism was attributed to the transferred charge from gas molecules to ZnO, which could further influence the luminescence signal of Eu^{3+}. Combined with the easy preparation, low cost and thermo-independent fluorescence, this material showed the potential in detecting aldehyde gases in vehicles.[142]

With ligands of 4,4′-oxybis(benzoate) acid (H_2OBA) and 3-amino-1,2,4-triazole (Hatz), a bimetallic EuTb-MOF was fabricated with dual emission peaks of Eu^{3+} and Tb^{3+}. The obtained mixed-Ln MOF could decode methanol *via* obvious colour change from light yellow to light green in solution and vaporous state. This specific response to methanol was explained by the modulated antenna effect with the addition of methanol, which could efficiently enhance the ligand-to-metal energy transfer from OBA^{2-} to Tb^{3+} and not influence that of OBA^{2-} to Eu^{3+}.[114]

Besides, Ln-MOFs were also applied in O_2 detection. A dual-emitting Eu-MOF film was prepared using an *in situ* growth

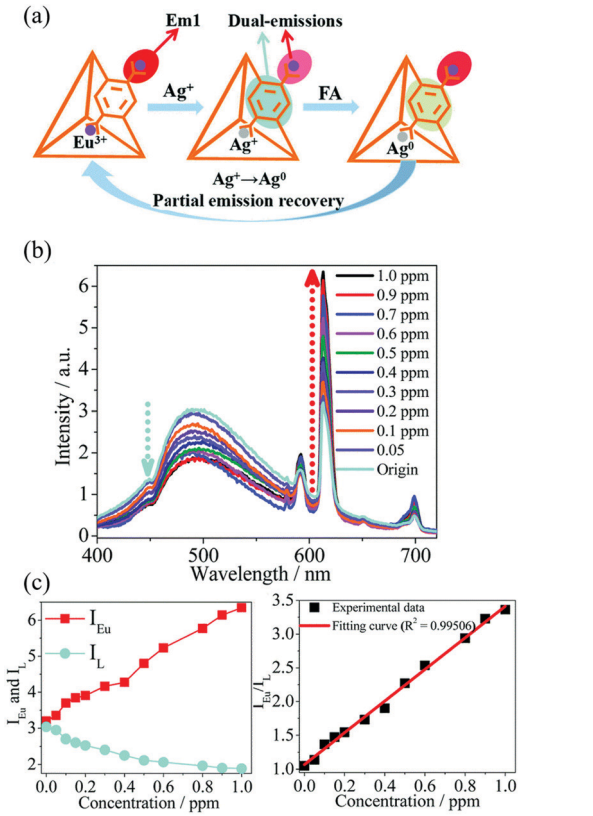

Fig. 16 (a) Schematic illustration of the mechanism of FA sensing by AgEu@UiO-66-COOH. (b) Concentration-dependent emission spectra and (c) the corresponding plots of the composite upon exposure to FA.[141] Reproduced from ref. 141 with permission from the Royal Society of Chemistry, copyright 2016.

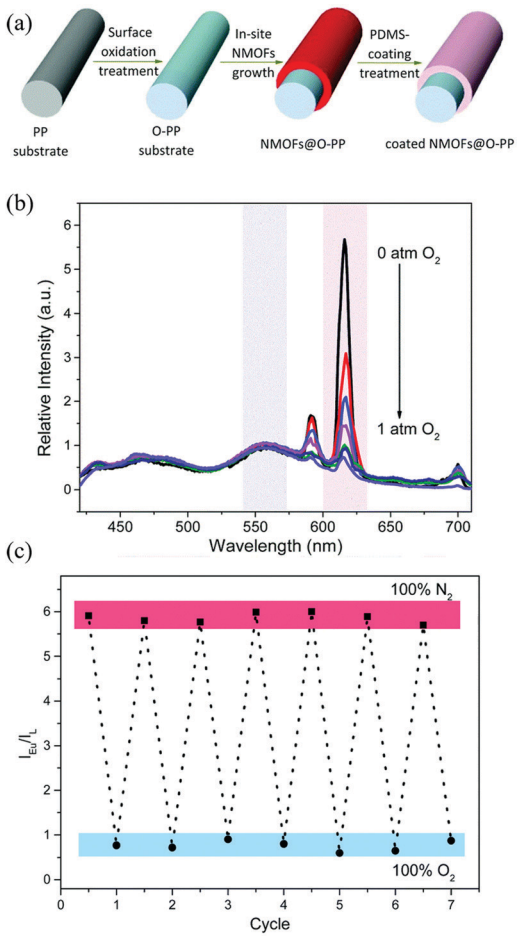

Fig. 17 Eu-MOF film for ratiometric and recycled oxygen sensing.[143] Reproduced from ref. 143 with permission from the Royal Society of Chemistry, copyright 2016.

method to load SUMOF-6-Eu on flexible nonwoven polypropylene (PP) and further coated by polydimethylsiloxane (PDMS). With the O_2-sensitive emission of Eu^{3+} and the reference emission from ligand H_2BPDC, this hybrid film demonstrated the O_2 sensing property, with high sensitivity (LOD 0.45%), good reusability, rapid response and recovery (10 s/60 s) (Fig. 17).[143]

4.4 Thermometer

Recently, luminescence thermometry has attracted much attention, due to its portable, noninvasive, and accurate detection performance. Ln-incorporated MOFs have been extensively explored in the construction of a thermometer, because a number of energy transfer processes within MOFs can be regulated by temperature. And the thermometrics developed by the strategies of mixed-Ln MOFs[63,104–106,108,109,116,144–148] or dye@Ln-MOFs[80,85,149] have been widely explored. With a new tetracarboxylic ligand, 2,6-di(2,4′-dicarboxylphenyl)pyridine, a series of binary EuTb-MOFs and ternary EuTbGd-MOFs were constructed for the ratiometric sensors and white light materials. Among them, the $Eu_{0.0066}Tb_{0.9934}$-MOF showed a linear response to temperature in the range of 77–450 K, with a maximum relative sensitivity of 3.76% K^{-1} (450 K). The highest S_m was reported to be 6.11% K^{-1} in the $Eu_{0.013}Tb_{0.060}Gd_{0.927}$-MOF. With the increase of temperature, the shorter lifetimes of Tb^{3+} and the longer lifetime of Eu^{3+} in these MOFs indicated a higher energy transfer of Tb–To–Eu, which made these materials temperature sensors with high sensitivity.[105] In 2019, the Eu/Tb-BTC MOF film was synthesized on a quartz substrate using a one-pot wet chemical method. The obtained film showed a temperature-dependent ratio of I_{Tb}/I_{Eu} as well as an emission change from green to red in the range of 298–383 K, which might originate from the elevated energy transfer from Tb^{3+} to Eu^{3+}. The optimized $Eu_{0.2}Tb_{0.98}$-MOF film exhibited a relatively high sensitivity of 16.14% K^{-1} at 359 K (Fig. 18).[108]

Besides, dual-signal dye@ZJU-88 was prepared by encapsulating perylene molecules in MOF's channels *via* ion exchange. The obtained composite could in-situ and exactly monitor the temperature in the physiological range (20–80 °C) with the S_m of 1.28% $°C^{-1}$ at 20 °C. With increasing temperature in this range, the emission intensity of the dye slowly decreased with the increasing signal of the Eu-MOF, which was attributed to the improved energy transfer from perylene to Eu^{3+}. With the high stability and low toxicology under the simulated physiological conditions, the composite showed potential as a ratiometric thermometer in the biological system.[80] Using the same strategy, a dye@Tb-MOF was built with a dye, C460

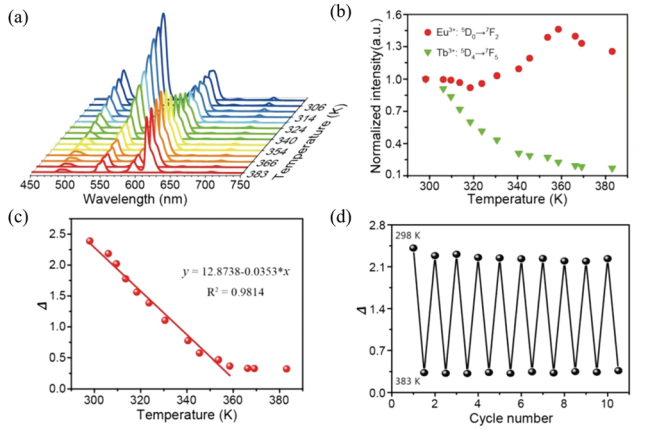

Fig. 18 (a) Emission spectra of the $Tb_{0.980}/Eu_{0.020}$-BTC film in the temperature range of 298–383 K under excitation of 296 nm. (b) Normalized emission intensity of Tb^{3+} and Eu^{3+} as a function of temperature. (c) Temperature dependence of the emission intensity ratio of Tb^{3+} to Eu^{3+}. (d) Cyclic stability of the film.[108] Reproduced from ref. 108 with permission from the Wiley, copyright 2019.

(7-diethylamino-4-methylcoumarin) through ion exchange. Upon excitation at 360 nm, the material owned both the emissions of Tb^{3+} and C460 (430 nm) and the intensity ratio changed linearly in the temperature from 50 K to 300 K. This specific thermos-response was attributed to the possible energy transfer from the dye to the Tb-MOF due to their partly overlapped emission. The relative sensitivity was calculated to be 4.484% K^{-1}.[149]

Liu's group designed a ligand, 1,4-bis(5-carboxy-1*H*-benzimidazole-2-yl)benzene, to build a dual-emitting Eu-MOF for the quantitative detection of temperature and humidity as a dual-functional material. With increasing temperature in the cryogenic range from 10 K to 150 K, the Eu-MOF exhibited a slightly decreased emission of the ligand and substantially quenched light of Eu^{3+}. The author deduced that the thermal vibration of the coordinated water around Eu ions could weaken the "antenna effect" of the ligand and quench the emission of Eu^{3+} with the increase of temperature. With the thermal-followed luminescence properties, this MOF could detect temperature with the S_m of 0.12% K^{-1} at 150 K.[150]

In addition, two layers of TbCo-MOF and TbDyCo-MOF materials were constructed using a ligand, 4-hydroxypyridine (4-OHpy). With different emissive centers (Tb^{III} green, Dy^{III} yellow, 4-OHpy blue, $[Co(CN)_6]^{3-}$ red), the emissions of these materials could be tuned within an extensive range. These two series of materials could be applied as colorimetric and ratiometric luminescence thermometers in the range of 120–300 K, due to the temperature-dependent energy transfer processes. With the linear relationship between I_{Tb}/I_{Dy} and temperature, the TbDyCo-MOF exhibited the ratiometric luminescence detection of temperature with the maximal thermal sensitivity of 2.2(3)% K^{-1} excited at 270 nm in a range of 120–200 K.[97]

4.5 pH detection

As a fundamental parameter, detecting the pH value in water and biological fluids can be applied in the analysis of water quality and monitoring some processes of cell metabolism and enzyme activity.[151,152] In 2017, a mixed-Ln MOF EuTb-Hdpda (H_4dpda: 4-(3,5-dicarboxyphenyl)pyridine-2,6-dicarboxylic acid) was developed as a self-referencing luminescent pH sensor. Based on the density functional theory (DFT) calculation, the pH-related luminescence properties were explained by the deprotonation of uncoordinated carboxyl groups of the ligand, which can modulate the energy level of the ligand and increase the energy transfer possibility from the ligand to Tb^{3+}. Thus, with the pH value varying from 3.90 to 7.50, the emission of Tb^{3+} enhances gradually with the invariable signal of Eu^{3+}.[153] Besides, with the help of the CTAB (cetyltrimethylammonium bromide) surfactant, a nanoscale EuTb(fum)(ox) MOF (fum: fumarate, ox: oxalate) was synthesized using the micro-emulsion method involving adjustable morphology and size. The obtained MOF was proved to be a ratiometric pH probe with the pH-dependent ratio of I_{Eu}/I_{Tb} in the range of 3.00–7.00. This behavior was attributed to the impeded ligand-to-metal ion energy transfer by hydrogen/hydroxyl ions and different pH-sensitivity of the f–f transition of Eu^{3+} and Tb^{3+}, which lead to the quenching emissions of these Ln^{3+} ions at different rates. The MTT (3-(4,5-dimethylthiazol-2-yl)-2,5-diphenyl-tetrazolium bromide) assay and optical microscopy testified its low cytotoxicity and good biocompatibility, which is very important for biological applications.[154]

In 2019, a nanocomposite, 1-HP@CoTb-DPA was developed for detecting the strong acidic pH values (0.3–7.8) with high sensitivity and rapid response (30 s). After analysing the ^{1}H NMR (nuclear magnetic resonance) spectra and theoretical calculations, the specific pH-response property was attributed to the formation of DPA–H^+ through the protonation of the nitrogen atom in DPA, which could promote the intramolecular charge transfer and quench the luminescence of the composite by weakening the "antenna effect" of the ligand. With the reference signal of the guest 1-HP, the fabricated MOF and MOF-based fiber paper were applied in visual point-of-care pH detection in acidic solutions and artificial human gastric juices as a ratiometric sensor.[83]

5. Conclusions and perspective

With high colour purity and characteristic emissions, Ln ions show the potential to construct optical materials and optical devices. Combined with the merits of tunable and highly porous frameworks, Ln-based dual/multiple-emitting MOFs have been widely explored as ratiometric probes in sensing ions, temperature, gases, biomolecules and so on. Through rational design or post-modification, the pore properties and active sites can be adjusted and further sensitivity and selectivity were reinforced.

Despite these advantages, there are still some issues that should be considered while exploring their applications. First, as sensing materials are usually applied in aqueous or organic phase, the stability of MOFs in solvents should be enforced for the real detection mechanism. Besides, the detection mechanism

should be investigated through thorough characterization even combined with theoretical analysis. The obtained underlying mechanisms and host–guest interactions can be further used in the property prediction and design of materials with specific functions. Thirdly, developing MOF-based films or membranes as portable devices is really meaningful for sensing real samples in daily life. Moreover, except the reported research studies, the sensing application of Ln-functionalized MOF-based probes can be further extended to other fields, like some disease biomarkers or toxins, which are closely related to human health.

Keeping these challenges in mind, we believe that the ratiometric Ln-MOF sensors with superior properties will be potentially developed and will hold a bright future in luminescence sensing.

Conflicts of interest

There are no conflicts to declare.

Acknowledgements

The work was financially supported by the National Natural Science Foundation of China (No. 21731002 and 21975104) and the Guangdong Major Project of Basic and Applied Research (2019B030302009).

Notes and references

1 H. Furukawa, K. E. Cordova, M. O'Keeffe and O. M. Yaghi, *Science*, 2013, **341**, 1230444.
2 M. O'Keeffe, *Chem. Soc. Rev.*, 2009, **38**, 1215–1217.
3 M. Bosch, S. Yuan, W. Rutledge and H. C. Zhou, *Acc. Chem. Res.*, 2017, **50**, 857–865.
4 J. Lee, O. K. Farha, J. Roberts, K. A. Scheidt, S. T. Nguyen and J. T. Hupp, *Chem. Soc. Rev.*, 2009, **38**, 1450–1459.
5 Y.-S. Kang, Y. Lu, K. Chen, Y. Zhao, P. Wang and W.-Y. Sun, *Coord. Chem. Rev.*, 2019, **378**, 262–280.
6 H. Li, L. Li, R.-B. Lin, W. Zhou, Z. Zhang, S. Xiang and B. Chen, *EnergyChem*, 2019, **1**, 100006.
7 H. Zeng, X.-J. Xie, M. Xie, Y.-L. Huang, D. Luo, T. Wang, Y. Zhao, W. Lu and D. Li, *J. Am. Chem. Soc.*, 2019, **141**, 20390–20396.
8 I. Abánades Lázaro and R. S. Forgan, *Coord. Chem. Rev.*, 2019, **380**, 230–259.
9 Q. Li, J. Y. Zheng, Y. Yan, Y. S. Zhao and J. Yao, *Adv. Mater.*, 2012, **24**, 4745–4749.
10 J. Wang, G. Liu and M. R. Jan, *J. Am. Chem. Soc.*, 2004, **126**, 3010–3011.
11 S. W. Thomas, G. D. Joly and T. M. Swager, *Chem. Rev.*, 2007, **107**, 1339–1386.
12 W. Lu, Z. Wei, Z.-Y. Gu, T.-F. Liu, J. Park, J. Park, J. Tian, M. Zhang, Q. Zhang and T. G. Iii, *Chem. Soc. Rev.*, 2014, **43**, 5561–5593.
13 M. Rieger, M. Wittek, P. Scherer, S. Löbbecke and K. Müller-Buschbaum, *Adv. Funct. Mater.*, 2018, **28**, 1704250.
14 S. Ji, Y. Chen, S. Zhao, W. Chen, L. Shi, Y. Wang, J. Dong, Z. Li, F. Li and C. Chen, *Angew. Chem., Int. Ed.*, 2019, **131**, 4315–4319.
15 D. Wu, Z. Zhang, X. Chen, L. Meng, C. Li, G. Li, X. Chen, Z. Shi and S. Feng, *Chem. Commun.*, 2019, **55**, 14918–14921.
16 Y. Zhao, H. Zeng, K. Wu, D. Luo, X.-W. Zhu, W. Lu and D. Li, *J. Mater. Chem. C*, 2020, **8**, 4385–4391.
17 S. Wu, H. Min, W. Shi and P. Cheng, *Adv. Mater.*, 2019, 1805871.
18 H. Q. Yin and X. B. Yin, *Acc. Chem. Res.*, 2020, **53**, 485–495.
19 Z. Zhao, Z. Zhang, C. Li, H. Wu, J. Wang and Y. Lu, *J. Mater. Chem. A*, 2018, **6**, 16164–16169.
20 T. He, Y. Z. Zhang, X. J. Kong, J. Yu, X. L. Lv, Y. Wu, Z. J. Guo and J. R. Li, *ACS Appl. Mater. Interfaces*, 2018, **10**, 16650–16659.
21 Y.-Z. Chen and H.-L. Jiang, *Chem. Mater.*, 2016, **28**, 6698–6704.
22 S. Wang, Q. Wang, X. Feng, B. Wang and L. Yang, *Adv. Mater.*, 2017, **29**, 1701898.
23 Y. Cui, F. Zhu, B. Chen and G. Qian, *Chem. Commun.*, 2015, **51**, 7420–7431.
24 H. Cai, W. Lu, C. Yang, M. Zhang, M. Li, C.-M. Che and D. Li, *Adv. Opt. Mater.*, 2019, **7**, 1801149.
25 H. Wang, W. P. Lustig and J. Li, *Chem. Soc. Rev.*, 2018, **47**, 4729–4756.
26 J. Dong, D. Zhao, Y. Lu and W.-Y. Sun, *J. Mater. Chem. A*, 2019, **7**, 22744–22767.
27 R. Gui, H. Jin, X. Bu, Y. Fu, Z. Wang and Q. Liu, *Coord. Chem. Rev.*, 2019, **383**, 82–103.
28 A. Pandey, N. Dhas, P. Deshmukh, C. Caro, P. Patil, M. Luisa García-Martín, B. Padya, A. Nikam, T. Mehta and S. Mutalik, *Coord. Chem. Rev.*, 2020, **409**, 213212.
29 F. Y. Yi, D. Chen, M. K. Wu, L. Han and H. L. Jiang, *ChemPlusChem*, 2016, **81**, 675–690.
30 J.-C. G. Bünzli and C. Piguet, *Chem. Soc. Rev.*, 2005, **34**, 1048–1077.
31 K. Binnemans, *Chem. Rev.*, 2009, **109**, 4283–4374.
32 K. Kuriki, Y. Koike and Y. Okamoto, *Chem. Rev.*, 2002, **102**, 2347–2356.
33 X. Yang, X. Lin, Y. Zhao, Y. S. Zhao and D. Yan, *Angew. Chem., Int. Ed.*, 2017, **56**, 7853–7857.
34 J.-C. G. Bünzli and S. V. Eliseeva, *J. Rare Earths*, 2010, **28**, 824–842.
35 Y. Hasegawa and Y. Kitagawa, *J. Mater. Chem. C*, 2019, **7**, 7494–7511.
36 B. Yan, *Acc. Chem. Res.*, 2017, **50**, 2789–2798.
37 A. J. Amoroso and S. J. A. Pope, *Chem. Soc. Rev.*, 2015, **44**, 4723–4742.
38 H. Xu, C. S. Cao, X. M. Kang and B. Zhao, *Dalton Trans.*, 2016, **45**, 18003–18017.
39 S.-N. Zhao, G. Wang, D. Poelman and P. Voort, *Materials*, 2018, **11**, 572.
40 Y. Gao, G. Yu, K. Liu and B. Wang, *Sens. Actuators, B*, 2018, **257**, 931–935.
41 X.-Y. Xu and B. Yan, *Sens. Actuators, B*, 2016, **222**, 347–353.

42 T. Gong, P. Li, Q. Sui, J. Chen, J. Xu and E.-Q. Gao, *J. Mater. Chem. A*, 2018, **6**, 9236–9244.
43 S. Wu, Y. Lin, J. Liu, W. Shi, G. Yang and P. Cheng, *Adv. Funct. Mater.*, 2018, **28**, 1707169.
44 N. Sun and B. Yan, *Sens. Actuators, B*, 2018, **261**, 153–160.
45 S.-J. Qin and B. Yan, *Sens. Actuators, B*, 2018, **259**, 125–132.
46 L. Guo, M. Liang, X. Wang, R. Kong, G. Chen, L. Xia and F. Qu, *Chem. Sci.*, 2020, **11**, 2407–2413.
47 J. Rocha, C. D. Brites and L. D. Carlos, *Chemistry*, 2016, **22**, 14782–14795.
48 D. Yue, D. Zhao, J. Zhang, L. Zhang, K. Jiang, X. Zhang, Y. Cui, Y. Yang, B. Chen and G. Qian, *Chem. Commun.*, 2017, **53**, 11221–11224.
49 D. Yue, Y. Huang, L. Zhang, K. Jiang, X. Zhang, Y. Cui, Y. Yu and G. Qian, *J. Mater. Chem. C*, 2018, **6**, 2054–2059.
50 R. L. White, *J. Appl. Phys.*, 1969, **40**, 1061–1069.
51 L. Tsonev, *Opt. Mater.*, 2008, **30**, 892–899.
52 G. Wang, Q. Peng and Y. Li, *Acc. Chem. Res.*, 2011, **44**, 322–332.
53 M. J. F. Digonnet, *Rare-earth-doped fiber lasers and amplifiers, revised and expanded*, CRC Press, 2001.
54 M. Peng, Y. Zhang, Y. Liu, M. Song, J. Zhai and Z. L. Wang, *Adv. Mater.*, 2014, **26**, 6767–6772.
55 X. Jiang, C. Cao, W. Feng and F. Li, *J. Mater. Chem. B*, 2016, **4**, 87–95.
56 C. Zhang, H. P. Zhou, L. Y. Liao, W. Feng, W. Sun, Z. X. Li, C. H. Xu, C. J. Fang, L. D. Sun and Y. W. Zhang, *Adv. Mater.*, 2010, **22**, 633–637.
57 J.-C. G. Bünzli, S. Comby, A.-S. Chauvin and C. D. B. Vandevyver, *J. Rare Earths*, 2007, **25**, 257–274.
58 P. Dorenbos, *J. Lumin.*, 2000, **91**, 91–106.
59 S. V. Eliseeva and J. C. G. Bünzli, *Basics of Lanthanide Photophysics*, 2011, vol. 7, pp. 1–45.
60 H. Yin, P. J. Carroll, B. C. Manor, J. M. Anna and E. J. Schelter, *J. Am. Chem. Soc.*, 2016, **138**, 5984–5993.
61 S. V. Eliseeva and J. C. Bunzli, *Chem. Soc. Rev.*, 2010, **39**, 189–227.
62 Z. Hu, B. J. Deibert and J. Li, *Chem. Soc. Rev.*, 2014, **43**, 5815–5840.
63 H. Li, W. Han, R. Lv, A. Zhai, X. L. Li, W. Gu and X. Liu, *Anal. Chem.*, 2019, **91**, 2148–2154.
64 T. Sun, P. Wang, R. Fan, W. Chen, S. Hao and Y. Yang, *J. Mater. Chem. C*, 2019, **7**, 3598–3606.
65 S. I. Weissman, *J. Chem. Phys.*, 1942, **10**, 214–217.
66 J.-C. G. Bünzli, *Coord. Chem. Rev.*, 2015, **293–294**, 19–47.
67 F. J. Steemers, W. Verboom, D. N. Reinhoudt, E. B. van der Tol and J. W. Verhoeven, *J. Am. Chem. Soc.*, 1995, **117**, 9408–9414.
68 H.-Q. Yin, X.-Y. Wang and X.-B. Yin, *J. Am. Chem. Soc.*, 2019, **141**, 15166–15173.
69 R. He, Y.-L. Wang, H.-F. Ma, S.-G. Yin and Q.-Y. Liu, *Dyes Pigm.*, 2018, **151**, 342–347.
70 L. Li, Y. Zhu, X. Zhou, C. D. S. Brites, D. Ananias, Z. Lin, F. A. A. Paz, J. Rocha, W. Huang and L. D. Carlos, *Adv. Funct. Mater.*, 2016, **26**, 8677–8684.
71 Y. Zhao, M.-Y. Wan, J.-P. Bai, H. Zeng, W. Lu and D. Li, *J. Mater. Chem. A*, 2019, **7**, 11127–11133.
72 A. Beeby, I. M. Clarkson, R. S. Dickins, S. Faulkner, D. Parker, L. Royle, A. S. de Sousa, J. A. G. Williams and M. Woods, *J. Chem. Soc., Perkin Trans. 2*, 1999, 493–504.
73 Y. Dong, J. Cai, Q. Fang, X. You and Y. Chi, *Anal. Chem.*, 2016, **88**, 1748–1752.
74 Y. Zhou, D. Zhang, W. Xing, J. Cuan, Y. Hu, Y. Cao and N. Gan, *Anal. Chem.*, 2019, **91**, 4845–4851.
75 B. Li, W. Wang, Z. Hong, E. M. El-Sayed and D. Yuan, *Chem. Commun.*, 2019, **55**, 6926–6929.
76 L. Yu, Q. Zheng, H. Wang, C. Liu, X. Huang and Y. Xiao, *Anal. Chem.*, 2020, **92**, 1402–1408.
77 Y. Wang, J. He, M. Zheng, M. Qin and W. Wei, *Talanta*, 2019, **191**, 519–525.
78 Y. Cui, T. Song, J. Yu, Y. Yang, Z. Wang and G. Qian, *Adv. Funct. Mater.*, 2015, **25**, 4796–4802.
79 T. Song, J. Yu, Y. Cui, Y. Yang and G. Qian, *Dalton Trans.*, 2016, **45**, 4218–4223.
80 Y. Cui, R. Song, J. Yu, M. Liu, Z. Wang, C. Wu, Y. Yang, Z. Wang, B. Chen and G. Qian, *Adv. Mater.*, 2015, **27**, 1420–1425.
81 Y. Gao, Y. Qi, K. Zhao, Q. Wen, J. Shen, L. Qiu and W. Mou, *Sens. Actuators, B*, 2018, **257**, 553–560.
82 K. Shi, Z. Yang, L. Dong and B. Yu, *Sens. Actuators, B*, 2018, **266**, 263–269.
83 L. Yu, Q. Zheng, D. Wu and Y. Xiao, *Sens. Actuators, B*, 2019, **294**, 199–205.
84 H. He, E. Ma, Y. Cui, J. Yu, Y. Yang, T. Song, C.-D. Wu, X. Chen, B. Chen and G. Qian, *Nat. Commun.*, 2016, **7**, 1–7.
85 D. Zhao, D. Yue, K. Jiang, Y. Cui, Q. Zhang, Y. Yang and G. Qian, *J. Mater. Chem. C*, 2017, **5**, 1607–1613.
86 S. Zhu, Q. Meng, L. Wang, J. Zhang, Y. Song, H. Jin, K. Zhang, H. Sun, H. Wang and B. Yang, *Angew. Chem., Int. Ed.*, 2013, **52**, 3953–3957.
87 J. Hao, F. Liu, N. Liu, M. Zeng, Y. Song and L. Wang, *Sens. Actuators, B*, 2017, **245**, 641–647.
88 M. Zhao, Y. Wang, Q. Ma, Y. Huang, X. Zhang, J. Ping, Z. Zhang, Q. Lu, Y. Yu, H. Xu, Y. Zhao and H. Zhang, *Adv. Mater.*, 2015, **27**, 7372–7378.
89 H. Weng and B. Yan, *Anal. Chim. Acta*, 2017, **988**, 89–95.
90 C. Liu, T. Wang, J. Ji, C. Wang, H. Wang, P. Jin, W. Zhou and J. Jiang, *J. Mater. Chem. C*, 2019, **7**, 10240–10246.
91 Y. Zhang, H. Yao, Y. Xu and Z. Xia, *Dyes Pigm.*, 2018, **157**, 321–327.
92 Z.-R. Yang, M.-M. Wang, X.-S. Wang and X.-B. Yin, *Anal. Chem.*, 2017, **89**, 1930–1936.
93 Y. Cui, F. Chen and X. B. Yin, *Biosens. Bioelectron.*, 2019, **135**, 208–215.
94 Q. Du, P. Wu, P. Dramou, R. Chen and H. He, *New J. Chem.*, 2019, **43**, 1291–1298.
95 H. Wang, X. Wang, M. Liang, G. Chen, R. M. Kong, L. Xia and F. Qu, *Anal. Chem.*, 2020, **92**, 3366–3372.
96 X. Zheng, R. Fan, Y. Song, K. Xing, P. Wang and Y. Yang, *ACS Appl. Mater. Interfaces*, 2018, **10**, 32698–32706.
97 K. Kumar, S. Chorazy, K. Nakabayashi, H. Sato, B. Sieklucka and S.-I. Ohkoshi, *J. Mater. Chem. C*, 2018, **6**, 8372–8384.
98 H. Weng and B. Yan, *Sens. Actuators, B*, 2017, **253**, 1006–1011.

99 C. Li, J. Huang, H. Zhu, L. Liu, Y. Feng, G. Hu and X. Yu, *Sens. Actuators, B*, 2017, **253**, 275–282.
100 J. X. Wu and B. Yan, *J. Colloid Interface Sci.*, 2017, **504**, 197–205.
101 Y. N. Zeng, H. Q. Zheng, J. F. Gu, G. J. Cao, W. E. Zhuang, J. D. Lin, R. Cao and Z. J. Lin, *Inorg. Chem.*, 2019, **58**, 13360–13369.
102 J. F. Feng, T. F. Liu, J. Shi, S. Y. Gao and R. Cao, *ACS Appl. Mater. Interfaces*, 2018, **10**, 20854–20861.
103 T. Xia, J. Wang, K. Jiang, Y. Cui, Y. Yang and G. Qian, *Chin. Chem. Lett.*, 2018, **29**, 861–864.
104 A. M. Kaczmarek, Y. Y. Liu, C. Wang, B. Laforce, L. Vincze, P. Van Der Voort and R. Van Deun, *Dalton Trans.*, 2017, **46**, 12717–12723.
105 Y. Yang, L. Chen, F. Jiang, M. Yu, X. Wan, B. Zhang and M. Hong, *J. Mater. Chem. C*, 2017, **5**, 1981–1989.
106 Y. Yang, H. Huang, Y. Wang, F. Qiu, Y. Feng, X. Song, X. Tang, G. Zhang and W. Liu, *Dalton Trans.*, 2018, **47**, 13384–13390.
107 Y. Su, J. Yu, Y. Li, S. F. Z. Phua, G. Liu, W. Q. Lim, X. Yang, R. Ganguly, C. Dang, C. Yang and Y. Zhao, *Commun. Chem.*, 2018, **1**, 12.
108 X. Yang, H. Zou, X. Sun, T. Sun, C. Guo, Y. Fu, C. M. L. Wu, X. Qiao and F. Wang, *Adv. Opt. Mater.*, 2019, **7**, 1900336.
109 D. Zhao, D. Yue, K. Jiang, L. Zhang, C. Li and G. Qian, *Inorg. Chem.*, 2019, **58**, 2637–2644.
110 Y. Zhang, B. Li, H. Ma, L. Zhang and Y. Zheng, *Biosens. Bioelectron.*, 2016, **85**, 287–293.
111 Y. Zhang, B. Li, H. Ma, L. Zhang, H. Jiang, H. Song, L. Zhang and Y. Luo, *J. Mater. Chem. C*, 2016, **4**, 7294–7301.
112 M.-L. Shen, B. Liu, L. Xu and H. Jiao, *J. Mater. Chem. C*, 2020, **8**, 4392–4400.
113 L. Li, J. Cheng, Z. Liu, L. Song, Y. You, X. Zhou and W. Huang, *ACS Appl. Mater. Interfaces*, 2018, **10**, 44109–44115.
114 D.-M. Chen, C.-X. Sun, Y. Peng, N.-N. Zhang, H.-H. Si, C.-S. Liu and M. Du, *Sens. Actuators, B*, 2018, **265**, 104–109.
115 X. Mi, D. Sheng, Y. Yu, Y. Wang, L. Zhao, J. Lu, Y. Li, D. Li, J. Dou, J. Duan and S. Wang, *ACS Appl. Mater. Interfaces*, 2019, **11**, 7914–7926.
116 X. Rao, T. Song, J. Gao, Y. Cui, Y. Yang, C. Wu, B. Chen and G. Qian, *J. Am. Chem. Soc.*, 2013, **135**, 15559–15564.
117 L. Ruiz-Garcia, L. Lunadei, P. Barreiro and I. Robla, *Sensors*, 2009, **9**, 4728–4750.
118 A. M. Kłonkowski, S. Lis, M. Pietraszkiewicz, Z. Hnatejko, K. Czarnobaj and M. Elbanowski, *Chem. Mater.*, 2003, **15**, 656–663.
119 S. G. Dunning, A. J. Nuñez, M. D. Moore, A. Steiner, V. M. Lynch, J. L. Sessler, B. J. Holliday and S. M. Humphrey, *Chem*, 2017, **2**, 579–589.
120 Y. Zhang, L. Chen, Z. Liu, W. Liu, M. Yuan, J. Shu, N. Wang, L. He, J. Zhang, J. Xie, X. Chen and J. Diwu, *ACS Appl. Mater. Interfaces*, 2020, **12**, 16648–16654.
121 M. A. Shenashen, S. A. El-Safty and E. A. Elshehy, *J. Hazard. Mater.*, 2013, **260**, 833–843.
122 K. P. Carter, A. M. Young and A. E. Palmer, *Chem. Rev.*, 2014, **114**, 4564–4601.
123 Y. Zhang and B. Yan, *Talanta*, 2019, **197**, 291–298.
124 B.-E. Kim, T. Nevitt and D. J. Thiele, *Nat. Chem. Biol.*, 2008, **4**, 176.
125 J. Wang, H. Chen, F. Ru, Z. Zhang, X. Mao, D. Shan, J. Chen and X. Lu, *Chem. – Eur. J.*, 2018, **24**, 3499–3505.
126 M. Harada, *Crit. Rev. Toxicol.*, 1995, **25**, 1–24.
127 X.-Y. Xu and B. Yan, *J. Mater. Chem. C*, 2016, **4**, 1543–1549.
128 X. Lian and B. Yan, *Dalton Trans.*, 2016, **45**, 18668–18675.
129 N.-N. Sun and B. Yan, *Dyes Pigm.*, 2017, **142**, 1–7.
130 D. Zhang, Y. Zhou, J. Cuan and N. Gan, *CrystEngComm*, 2018, **20**, 1264–1270.
131 S.-J. Qin and B. Yan, *Sens. Actuators, B*, 2018, **272**, 510–517.
132 G. C. Barrett and D. T. Elmore, *Amino acids and peptides*, Cambridge University Press, 1998.
133 G. F. Webb, *Proc. Natl. Acad. Sci. U. S. A.*, 2003, **100**, 4355.
134 K. Ai, B. Zhang and L. Lu, *Angew. Chem., Int. Ed.*, 2009, **48**, 304–308.
135 P. M. Pellegrino, N. F. Fell, D. L. Rosen and J. B. Gillespie, *Anal. Chem.*, 1998, **70**, 1755–1760.
136 D. Swierczynska-Machura, S. Brzeznicki, E. Nowakowska-Swirta, J. Walusiak-Skorupa, T. Wittczak, W. Dudek, M. Bonczarowska, W. Wesolowski, S. Czerczak and C. Palczynski, *Occupational exposure to diisocyanates in polyurethane foam factory workers*, 2015.
137 N. S. Palikhe, J.-H. Kim and H.-S. Park, *Allergy, Asthma Immun. Res.*, 2011, **3**, 21–26.
138 D. Giuliani, A. Ottani, D. Zaffe, M. Galantucci, F. Strinati, R. Lodi and S. Guarini, *Neurobiol. Learn. Mem.*, 2013, **104**, 82–91.
139 X. Zheng, R. Fan, Y. Song, A. Wang, K. Xing, X. Du, P. Wang and Y. Yang, *J. Mater. Chem. C*, 2017, **5**, 9943–9951.
140 J. Gao, Q. Li, C. Wang and H. Tan, *Sens. Actuators, B*, 2017, **253**, 27–33.
141 J. N. Hao and B. Yan, *Nanoscale*, 2016, **8**, 12047–12053.
142 X.-Y. Xu and B. Yan, *J. Mater. Chem. A*, 2017, **5**, 2215–2223.
143 X.-Y. Xu and B. Yan, *J. Mater. Chem. C*, 2016, **4**, 8514–8521.
144 Y. Cui, H. Xu, Y. Yue, Z. Guo, J. Yu, Z. Chen, J. Gao, Y. Yang, G. Qian and B. Chen, *J. Am. Chem. Soc.*, 2012, **134**, 3979–3982.
145 Y. Cui, W. Zou, R. Song, J. Yu, W. Zhang, Y. Yang and G. Qian, *Chem. Commun.*, 2014, **50**, 719–721.
146 Y. Wei, R. Sa, Q. Li and K. Wu, *Dalton Trans.*, 2015, **44**, 3067–3074.
147 D. Zhao, D. Yue, L. Zhang, K. Jiang and G. Qian, *Inorg. Chem.*, 2018, **57**, 12596–12602.
148 A. M. Kaczmarek, *J. Mater. Chem. C*, 2018, **6**, 5916–5925.
149 T. Xia, T. Song, Y. Cui, Y. Yang and G. Qian, *Dalton Trans.*, 2016, **45**, 18689–18695.
150 D. Wang, Q. Tan, J. Liu and Z. Liu, *Dalton Trans.*, 2016, **45**, 18450–18454.
151 X. Zhang, S. Rehm, M. M. Safont-Sempere and F. Würthner, *Nat. Chem.*, 2009, **1**, 623–629.
152 F. Cao, E. Ju, C. Liu, W. Li, Y. Zhang, K. Dong, Z. Liu, J. Ren and X. Qu, *Nanoscale*, 2017, **9**, 4128–4134.
153 T. Xia, Y. Cui, Y. Yang and G. Qian, *ChemNanoMat*, 2017, **3**, 51–57.
154 T. Xia, F. Zhu, K. Jiang, Y. Cui, Y. Yang and G. Qian, *Dalton Trans.*, 2017, **46**, 7549–7555.

